
Supplementary information

Facile synthesis of per(6-O-tert-butyltrimethylsilyl)- α -, β -, and γ -cyclodextrin as protected intermediates for the functionalization of the secondary face of the macrocycles

In the format provided by the authors and unedited

Facile synthesis of per(6-*O*-*tert*-butyldimethylsilyl)- α -, β -, and γ -cyclodextrin as protected intermediates for the functionalization of the secondary face of the macrocycles.

Gábor Benkovics¹, Milo Malanga¹, Giovanna Cutrone², Szabolcs Béni³, Antonio Vargas-Berenguel² & Juan Manuel Casas-Solvas^{2*}

¹CycloLab Kft., 09.ker. Illatos út 7, H-1097 Budapest, Hungary. E-mail: benkovics@cyclolab.hu (G.B.), malanga@cyclolab.hu (M.M.).

²Department of Chemistry and Physics, University of Almería, Carretera de Sacramento s/n, E-04120 Almería, Spain. E-mail: cutrone@ual.es (G.C.), avargas@ual.es (A.V.-B).

³Department of Pharmacognosy, Semmelweis University, Budapest, H-1085 Üllői út 26, Hungary. E-mail: beni.szabolcs@pharma.semmelweis-univ.hu (S.B.).

*E-mail: jmcasas@ual.es (J.M.C.-S.).

Supplementary Information

Table of Contents

I.	Equipment further details	S2-S3
II.	Alternative glassware setup for small scale (< 5 g of starting material)	S3-S5
III.	Reaction pictures for the silylation process of α -, β - and γ -CD in different solvents	S6-S9
IV.	Flash column chromatography setup	S10
V.	TLC monitoring of the reactions and the purification processes	S11-S13
VI.	HPLC monitoring of the reactions, the purification processes and purity assessment of the products	S14-S17
VII.	NMR, MALDI and IR spectra for hexakis(6- <i>O</i> -TBDMS)- α -CD 1	S18-S21
VIII.	NMR, MALDI and IR spectra for heptakis(6- <i>O</i> -TBDMS)- β -CD 2	S22-S24
IX.	NMR, MALDI and IR spectra for octakis(6- <i>O</i> -TBDMS)- γ -CD 3	S25-S30
X.	NMR, MALDI and IR spectra for oversilylated α -CD derivative	S31-S34
XI.	NMR, MALDI and IR spectra for oversilylated β -CD derivative	S35-S38
XII.	NMR, MALDI and IR spectra for oversilylated γ -CD derivative	S39-S41

I. Equipment further details

Thin layer chromatography (TLC) was performed on Merck silica gel 60 F₂₅₄ aluminum sheets and developed by 5% v/v sulfuric acid in ethanol. Flash column chromatography was performed on Merck silica gel (230–400 mesh, ASTM). Melting points were measured on a Büchi B-21 450 melting point apparatus and are uncorrected. Optical rotations were recorded on a Jasco P-1030 polarimeter at room temperature. $[\alpha]_D$ values are given in 10⁻¹ deg cm⁻¹ g⁻¹. Infrared spectra were recorded as KBr disks on a Perkin Elmer FTIR spectrometer Spectrum RX1. NMR experiments were carried out on a 600 MHz Varian DDR NMR spectrometer equipped with a 5 mm inverse-detection gradient (IDPFG) probehead, or on a Bruker Avance III HD 600 MHz spectrometer equipped with a QCI ¹H/¹³C/¹⁵N/³¹P proton-optimized quadrupole inverse cryoprobe with ¹H and ¹³C cryochannels. Standard pulse sequences and processing routines available in VnmrJ 3.2 C/Chempack 5.1, or Bruker TopSpin 3.6.2, respectively, were used for structure identifications. The complete resonance assignments were established from direct ¹H–¹³C, long-range ¹H–¹³C, and scalar spin–spin connectivities derived from 1D ¹H, ¹³C, 1D TOCSY, 2D ¹H–¹H gCOSY, 2D zTOCSY, 2D ¹H–¹³C gHSQCAD, and 2D ¹H–¹³C gHMBCAD experiments, respectively. The probe temperature was maintained at 298 K and standard 5 mm NMR tubes were used. Chemical shifts (δ) are given in parts per million (ppm) and referenced to the NMR solvents residual signals, CDCl₃ ($\delta_{1H} = 7.26$ ppm, $\delta_{13C} = 77.16$ ppm), THF-d₈ ($\delta_{1H} = 3.58$ and 1.73 ppm, $\delta_{13C} = 67.57$ and 25.37 ppm), or dimethyl sulfoxide-d₆ ($\delta_{1H} = 2.50$ ppm, $\delta_{13C} = 39.52$ ppm). *J* values are given in hertz (Hz). MALDI-TOF mass spectra were recorded on a 4800 Plus AB SCIEX spectrometer with 2,5-dihydroxybenzoic acid (DHB) as the matrix. HPLC measurements were performed on an Agilent 1260 Infinity HPLC system equipped with UV detector (Agilent 1200 Series Diode Array Detector, G1315B) coupled to refractive index (RI) detector (Agilent 1260 Infinity Refractive Index Detector + 8 μ L flowcell, G1362A) or with UV detector coupled to

evaporative light scattering detector (ELSD), (Agilent 385 G4261A). These setups were used to determine the purity of all cyclodextrin derivatives. The purity assessment of the final compounds and the monitoring of the purification process was performed on a Luna C18 250 mm × 4.6 mm, 5 μm (Phenomenex Inc., Torrance, CA, USA) analytical column with the mobile phase of methanol:ethylacetate (78:22), isocratic elution at a flow rate of 1.8 mL/min and with RI detection. Reaction monitoring was performed by using the same HPLC method, but using the ELSD.

II. Alternative glassware setup for small scale (< 5 g of starting material)

Equipment

- Borosilicate two-necked, round bottom flask with central NS 29/32 and lateral NS 14/23 sintered necks (250 mL; Pobel, cat. no. 0100108452)
- Teflon-coated magnetic stirring bar (2 cm length)
- Turn-over flange rubber NS 29/32 and NS 14/23 stoppers (Saint-Gobain performance plastics, cat. no. DX407030-05 and DX407015-20, respectively)
- Nitrogen gas supply equipped with a Drierite™ gas-drying unit (Aldrich, cat. no. Z112879-1EA) and a silicone tube ending in a syringe needle
- Gas bubbler (Fisher Scientific, cat. no. 31-500-701) filled with mineral or silicone oil and equipped with a silicone tube ending in a syringe needle
- Disposable 5 mL polypropylene 2-part syringes with Luer tip (Becton Dickinson, model BD Discardit® II)
- Disposable 0.8×50 mm hypodermic Luer syringe needles (Terumo, cat. no. NN-2150R)
- Latex balloons (wall thickness 10 mil; Merck, cat. No. Z154970)
- Laboratory film (Parafilm®)

Balloon syringe assembly:^{1,2} Remove the plunger of a 5 mL plastic syringe and cut-off the top half of the barrel. Insert 1.5-2 cm of the syringe bottom half into a helium quality latex balloon and seal the connection between both pieces by a band of laboratory film 2 cm in wide. Purge the balloon by inflating it with a nitrogen tubing supply through the syringe Luer tip followed by deflation. Repeat the inflating and deflating cycle three times. Finally inflate the balloon with nitrogen and attach a disposable Luer needle to the syringe. The balloon syringe assembly is ready for use. While transporting or waiting to be used, the assembly can be kept inflated by inserting the needle into a cork ring or a solid rubber stopper.

1 Place a Teflon-coated magnetic stirring bar into a 250 mL two-necked, round bottom flask, and cap the necks with turn-over flange stoppers.

2 Run a dry nitrogen gas flow within the flask through the lateral 14/23 neck using the needle-provided nitrogen supply as inlet and the needle-provided glass bubbler as outlet for 2 min (Supplementary Fig. 1A).

3 Keep the gas flow while removing the rubber stopper from the central neck. Add the required amount of previously dried CD and the solvent. Place the rubber stopper back.

4 Stop the gas flow and remove the nitrogen inlet and the gas bubbler from the lateral neck. Place the inflated balloon syringe assembly on the central neck (Supplementary Fig. 1B) and stir the suspension until a clear solution is formed (usually 30 min).

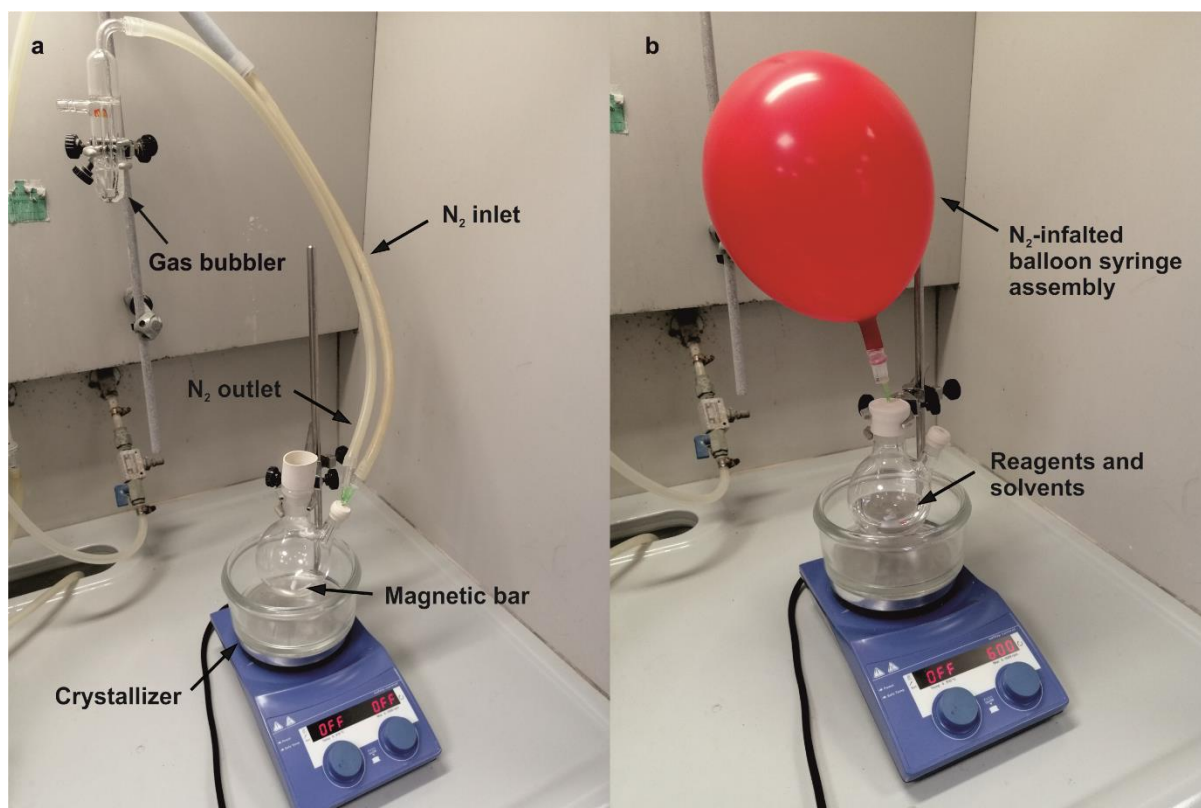
5 Run a gas flow through the lateral neck as described in Step 2.

6 Remove the balloon syringe and the rubber stopper from the central neck. Add the required amount of TBDMSCl into the flask. Place the rubber stopper and the balloon syringe back to the central neck.

¹ Boháč, A. A transferable gas container (TGC): improving the balloon inert atmosphere technique. *J. Chem. Educ.* **72**, 263 (1995). DOI: 10.1021/ed072p263.

² Pavia, D. L., Lampman, G. M., Kriz, G. S. & Engel, R. G. *A small scale approach to organic laboratory techniques*, Edn. 3, pp. 617-619 (Brooks/Cole, Belmont, California, USA, 2011).

7 Stop the gas flow and remove the nitrogen inlet and the gas bubbler from the lateral neck.



Supplementary Figure 1. A) Glassware setup during dry nitrogen gas flow through the lateral neck before adding the macrocycle and the solvent. B) Glassware setup with a balloon syringe assembly once the macrocycle and the solvent have been added.

III. Reaction pictures for the silylation process of α -, β - and γ -CD in different solvents

III.a. Silylation of α -CD



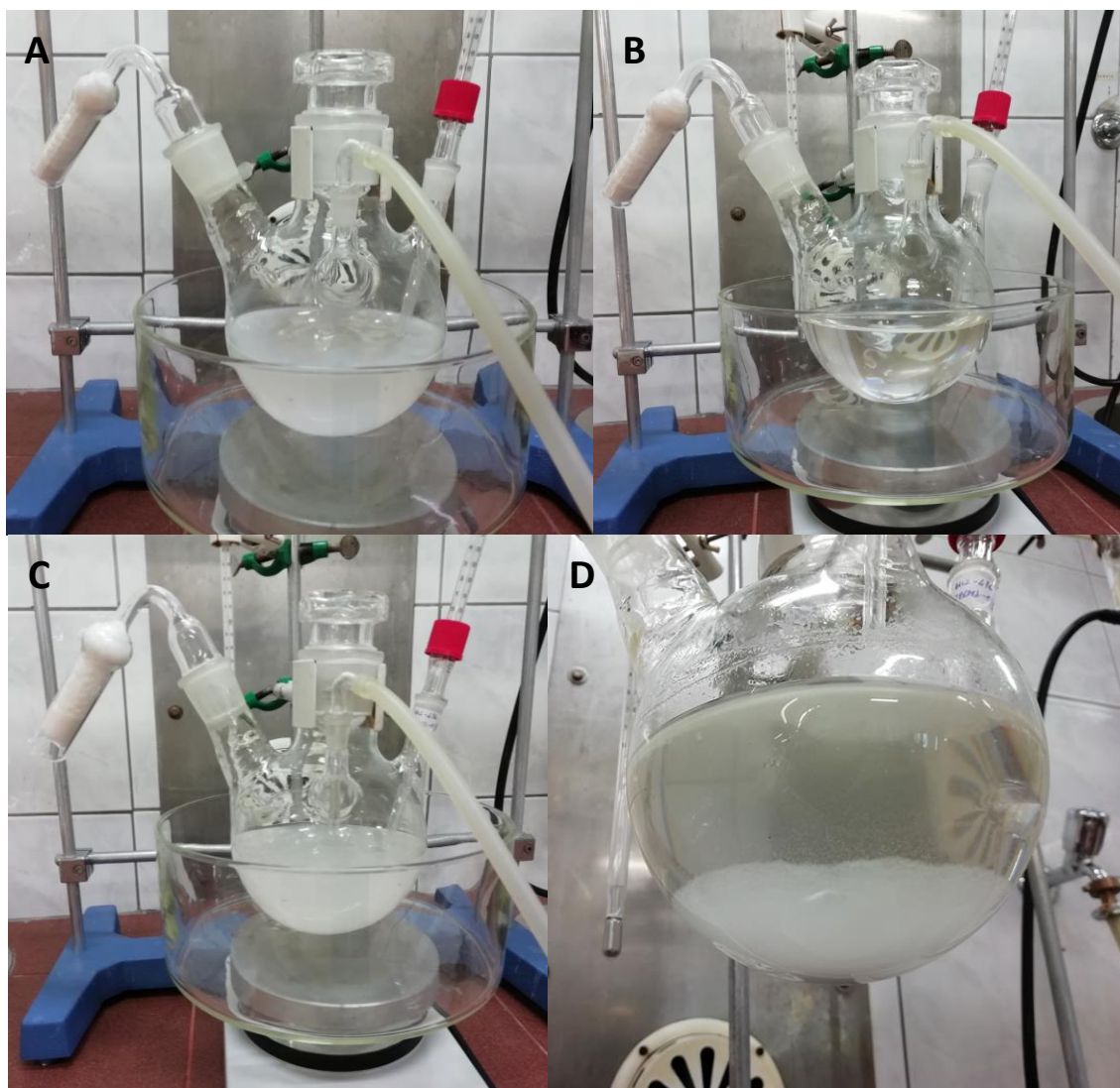
Supplementary Figure 2. A) α -CD is hardly soluble in pure pyridine, and a slightly cloudy solution is initially obtained. B) However, an abundant precipitate forms after ~15 min, probably due to the complexation with the solvent. C) In contrast, a clear solution can be observed when a 5:1 DMF-pyridine mixture is used. D) This situation does not change 12 h after the addition of TBDMSCl.

III.b. Silylation of β -CD



Supplementary Figure 3. **A)** β -CD readily dissolves in pure pyridine and gives a clear solution after \sim 30 min. **B)** This situation remains 12 h after the addition of TBDMSCl.

III.c. Silylation of γ -CD

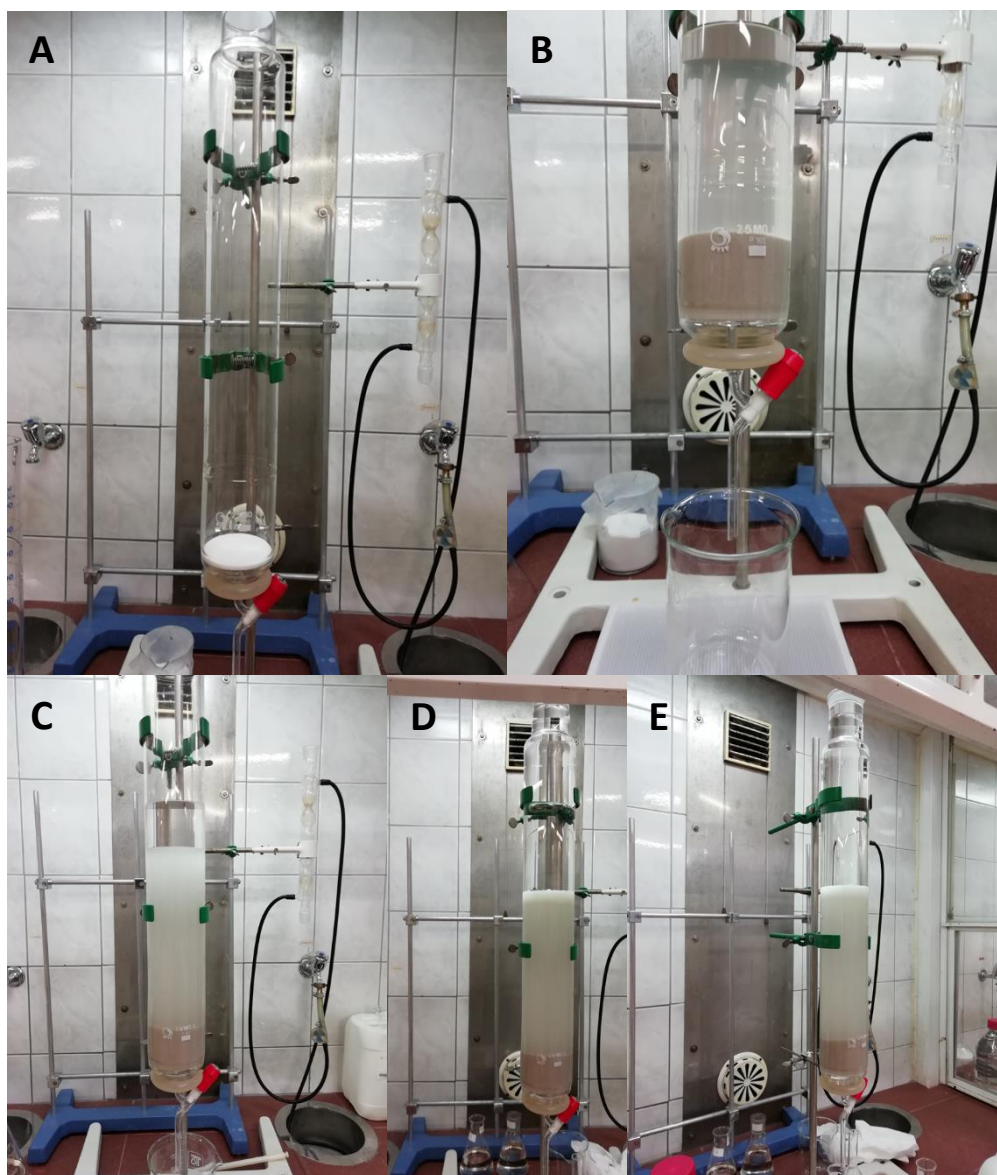


Supplementary Figure 4. A) γ -CD is hardly soluble in pure pyridine and forms a cloudy suspension with violet reflection with no detectable solid by naked eye. B) Addition of TBDMSCl makes the suspension clear. C and D) However, after 12 h stirring an abundant precipitate forms.



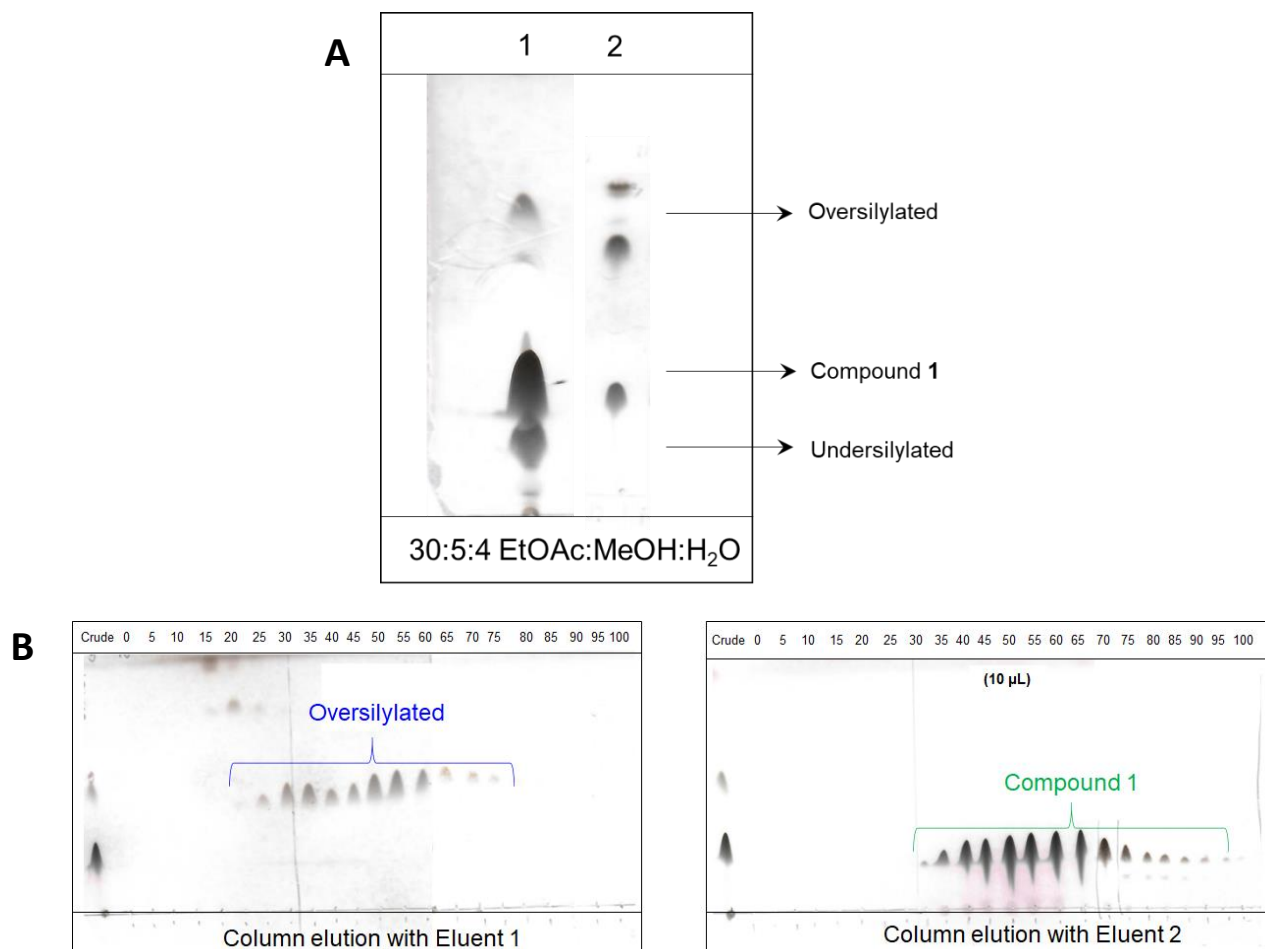
Supplementary Figure 4 (cont.). **E)** Addition of CH_2Cl_2 (in 1:4 ratio respect to pyridine) to the suspension showed in Supplementary Fig. 4C and D makes the suspension clear after 5 min. TLC showed that reaction was not complete. **F)** Addition of an extra portion of TBDMSCl initially keeps the solution clear. **G)** But after 12 h, compound **3** and the oversilylated species abundantly precipitate. TLC of the supernatant revealed that no undersilylated species were present.

IV. Flash column chromatography setup

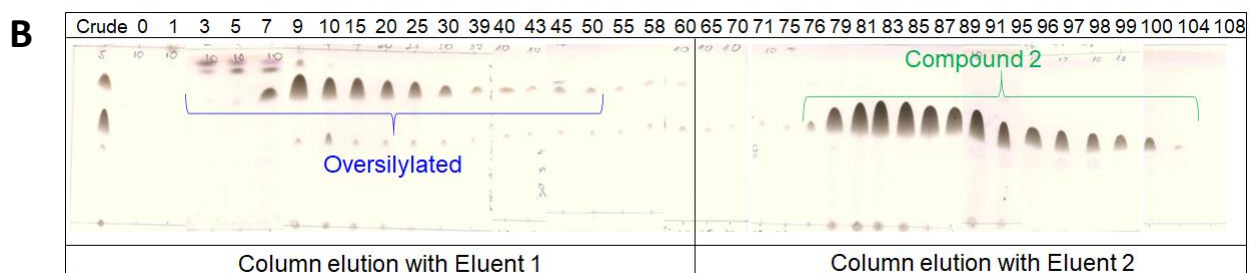
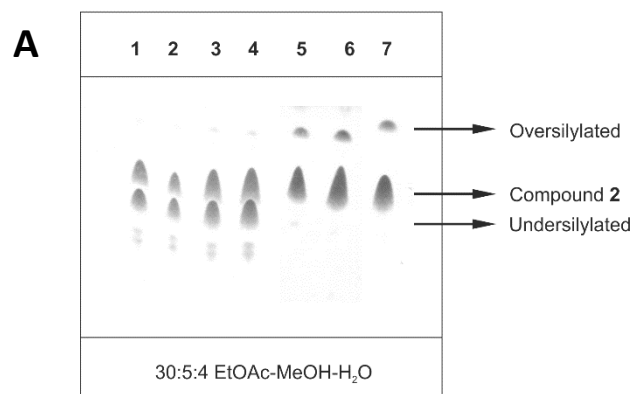


Supplementary Figure 5. A) Empty column. B) Sand pad. C) Conditioned column after the addition of the silica-solvent slurry onto the sand pad and the elution of the excess of solvent (note a short solvent layer at the top). D) Column loaded with the sample after eluting the excess of solvent (keep the silica always moistened). E) Column elution.

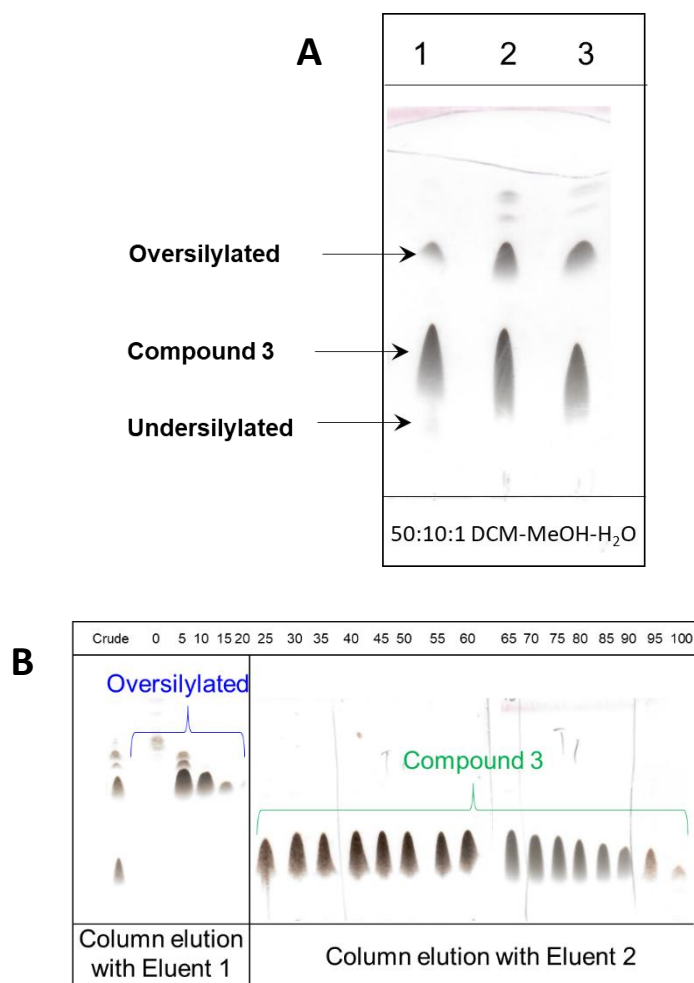
V. TLC monitoring of the reactions and the purification processes



Supplementary Figure 6. **A)** Silylation progress for α -CD as monitored by TLC (30:5:4 EtOAc-MeOH-H₂O) after the initial addition of TBDMSCI (line 1: 12 h), and after the addition of an extra portion of TBDMSCI (line 2: 12+12 h). Line 1 sample is 4 times more concentrated than line 2 sample. As can be seen, R_f values are concentration dependent. R_f values in Line 1: 0.13 for undersilylated species, 0.28 for compound **1**, and 0.62 for oversilylated species. **B)** Purification process of hexakis(6-*O*-*tert*-butyldimethylsilyl)- α -CD (**1**) as monitored by TLC (30:5:4 EtOAc-MeOH-H₂O) during the elution of the column with 40:40:20:4 CH₂Cl₂-MeCN-96% v/v EtOH-25% v/v aqueous NH₃ (Eluent 1: elution of oversilylated species) and 40:40:20:4 CH₂Cl₂-MeCN-96% v/v EtOH-H₂O (Eluent 2: elution of desired product **1**). Volume for each fraction is 200 mL.



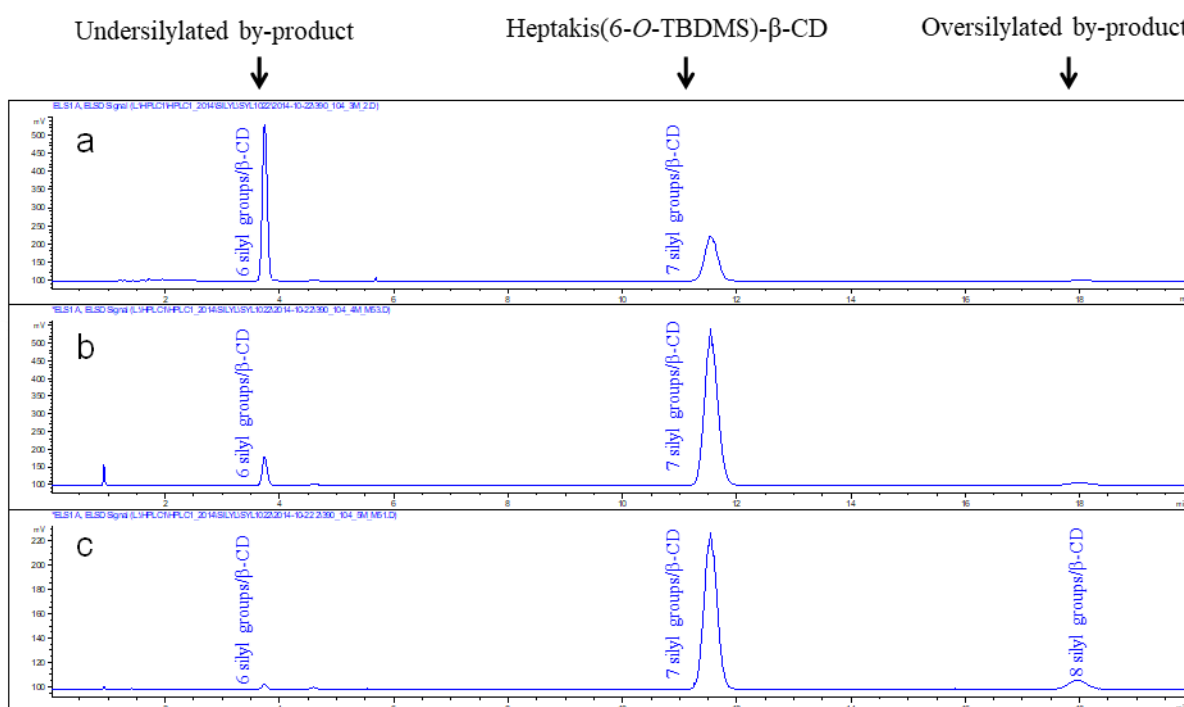
Supplementary Figure 7. A) Silylation progress for β -CD as monitored by TLC (30:5:4 EtOAc-MeOH-H₂O) after the initial addition of TBDMSCl (line 1: 1 h; line 2: 3 h; line 3: 6 h; line 4: 12 h), and after the addition of an extra portion of TBDMSCl (line 5: 12+12 h; line 6: 12+18 h; line 7: 12+24 h). R_f values in Line 5: 0.43 for undersilylated species, 0.54 for compound **2**, and 0.78 for oversilylated species. **B)** Purification process of heptakis(6-*O*-*tert*-butyldimethylsilyl)- β -CD (**2**) as monitored by TLC (30:5:4 EtOAc-MeOH-H₂O) during the elution of the column with 40:40:20:4 CH₂Cl₂-MeCN-96% v/v EtOH-25% v/v aqueous NH₃ (Eluent 1: elution of oversilylated species) and 40:40:20:4 CH₂Cl₂-MeCN-96% v/v EtOH-H₂O (Eluent 2: elution of desired product **2**). Volume for each fraction is 200 mL.



Supplementary Figure 8. **A**) Silylation progress for γ -CD as monitored by TLC (50:10:1 CH₂Cl₂-MeOH-H₂O) after the initial addition of TBDMSCl (line 1: 12 h), and after the addition of an extra portion of TBDMSCl (line 2: 12 h; line 3: 24 h). R_f values in Line 1: 0.18 for undersilylated species, 0.37 for compound **3**, and 0.58 for oversilylated species. **B**) Purification process of octakis(6-*O*-*tert*-butyldimethylsilyl)- γ -CD (**3**) as monitored by TLC (50:10:1 CH₂Cl₂-MeOH-H₂O) during the elution of the column with 50:15:1 CH₂Cl₂-MeOH-25% v/v aqueous NH₃ (Eluent 1: elution of oversilylated species) and 50:7:1 CH₂Cl₂-MeOH-H₂O (Eluent 2: elution of desired product **3**). Volume for each fraction is 250 mL.

VI. HPLC monitoring of the reactions, the purification processes and purity assessment of the products

The silylation at the primary side of the macrocycles and the crude purification were monitored by TLC and HPLC. The reaction proceeding was evaluated by qualitatively by HPLC with an isocratic elution (78:22 MeOH:EtOAc mobile phase) with a flow rate of 1.8 mL/min and C18 stationary phase with ELSD detection. In Supplementary Fig. 9 the reaction monitoring for the preparation of heptakis(6-*O*-TBDMS- β -CD) is shown as example.

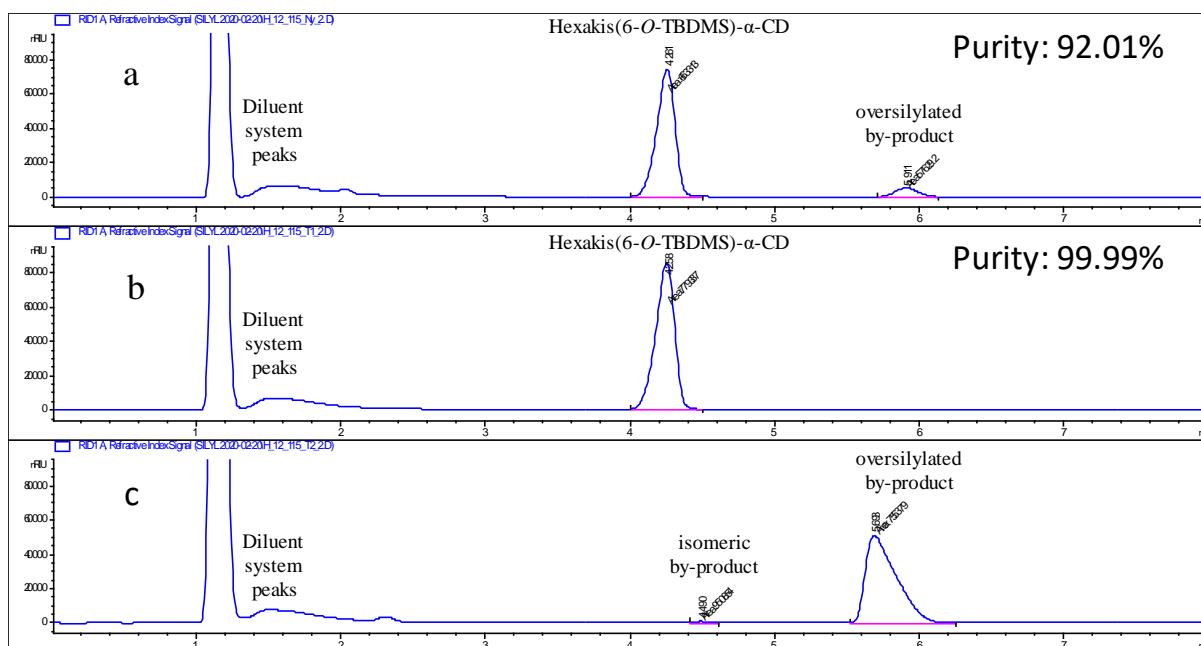


Supplementary Figure 9. Reaction monitoring of β -CD silylation by HPLC-ELSD: a) 1.0 equiv. of TBDMSCl per OH-6 group. b) 1.10 equiv. of TBDMSCl per OH-6 group. c) 1.25 equiv. of TBDMSCl per OH-6 group.

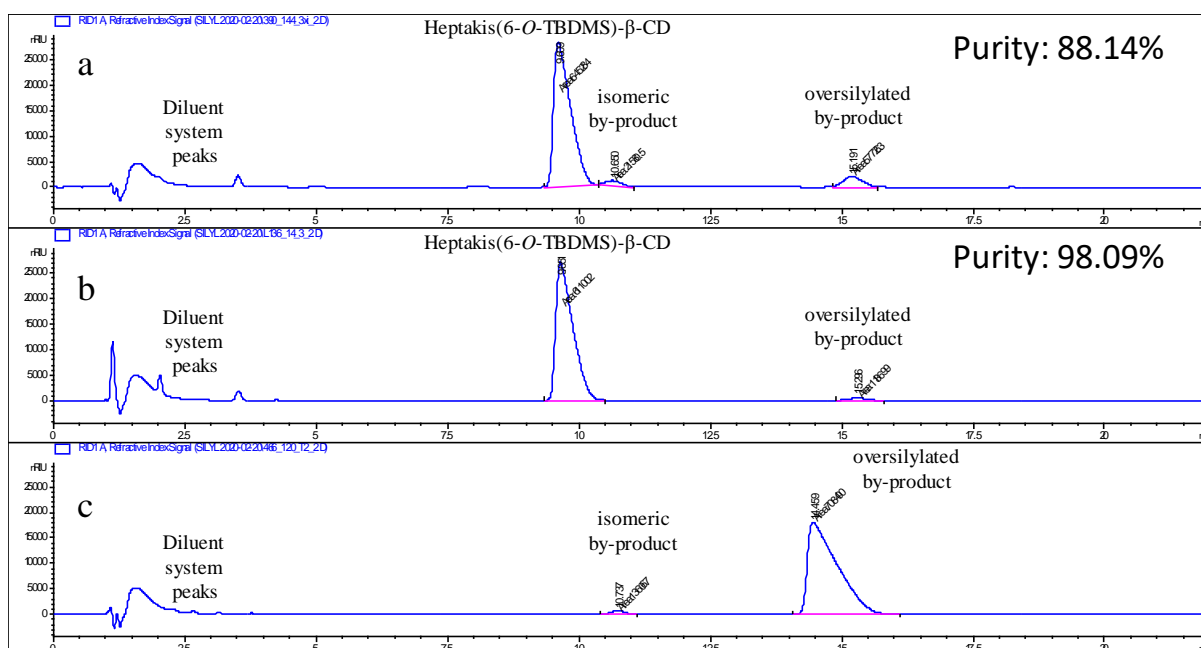
The ELSD detector can be used as a complementary qualitative analytical technique to TLC as it gives satisfactory resolution, of the target compound from the under- and over-silylated by-products. Nevertheless, because of the non-linear response vs concentration characteristics of

this detector and because of the unavailability of reference materials for each of the impurities, direct comparison of peak area values from the ELSD chromatogram might lead to false results and therefore for quantitative purposes this detection mode is not adequate. RID on the other hand is a universal detector in HPLC as it responds to every component in the mixture with consistent response factor and therefore it can be used to compare the area values of different peaks from the chromatogram. Final purity is therefore given as Area% value calculated from the integrated RID chromatograms. The disadvantage of the RI detector is its high sensitivity for minute changes in the mobile phase composition (gradient elution for example must be avoided). For this reason, for reaction monitoring when the samples are taken from constantly changing environment with different solvent and reagent compositions, RI detection cannot be applied as system peaks would give distorted baseline and would overlap with those of interest. In this scenario, the ELS detection mode must be used instead.

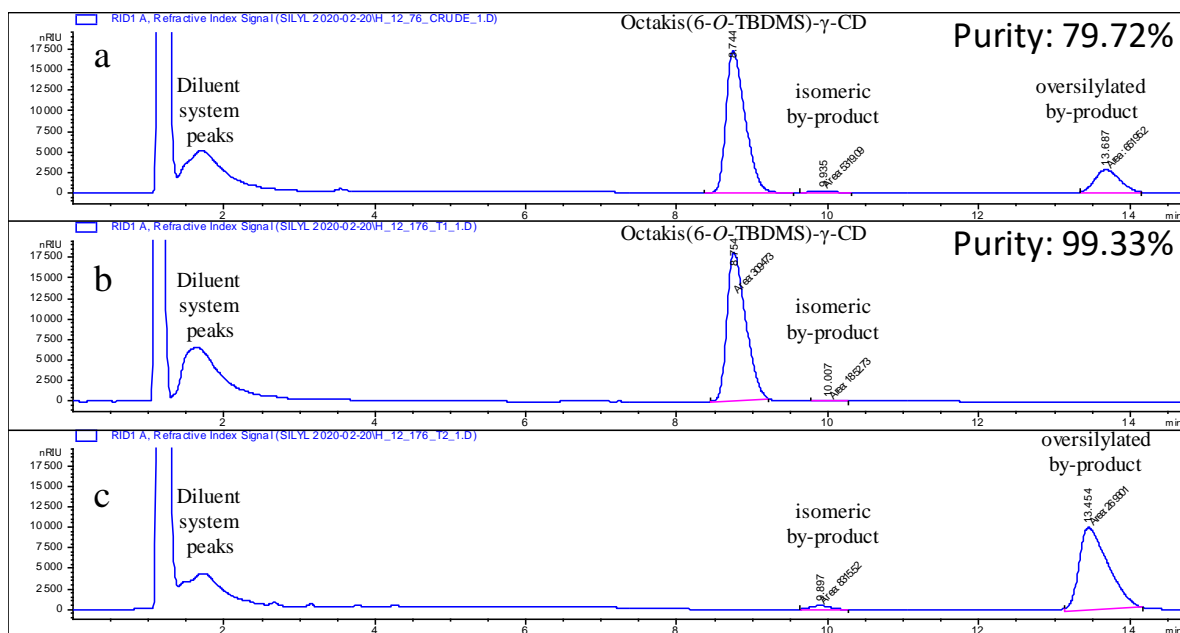
For the monitoring of the purification process (Supplementary Fig. 10-12) and for the determination of the isomeric purity of the target compounds, the non-aqueous isocratic reversed-phase HPLC method using Luna C18 column and RI detector was used. In these cases the reaction crude, the purified target compound and the isolated impurities (mainly over-silylated species) were solid materials, soluble in the elution mixture (78:22 MeOH:EtOAc), therefore the RI detection mode could be applied. Based on Area% evaluation of the RID chromatogram the isomeric purity of hexakis(6-*O*-TBDMS)- α -CD was 99.99% (Supplementary Fig. 10b), the isomeric purity of heptakis(6-*O*-TBDMS)- β -CD was 98.09% (Supplementary Fig. 11b), while the isomeric purity of octakis(6-*O*-TBDMS)- γ -CD was 99.33% (Supplementary Fig. 12b).



Supplementary Figure 10. Monitoring of the purification process of hexakis(6-*O*-TBDMS)- α -CD by HPLC-RID: a) reaction crude b) purified target compound c) isolated impurities.

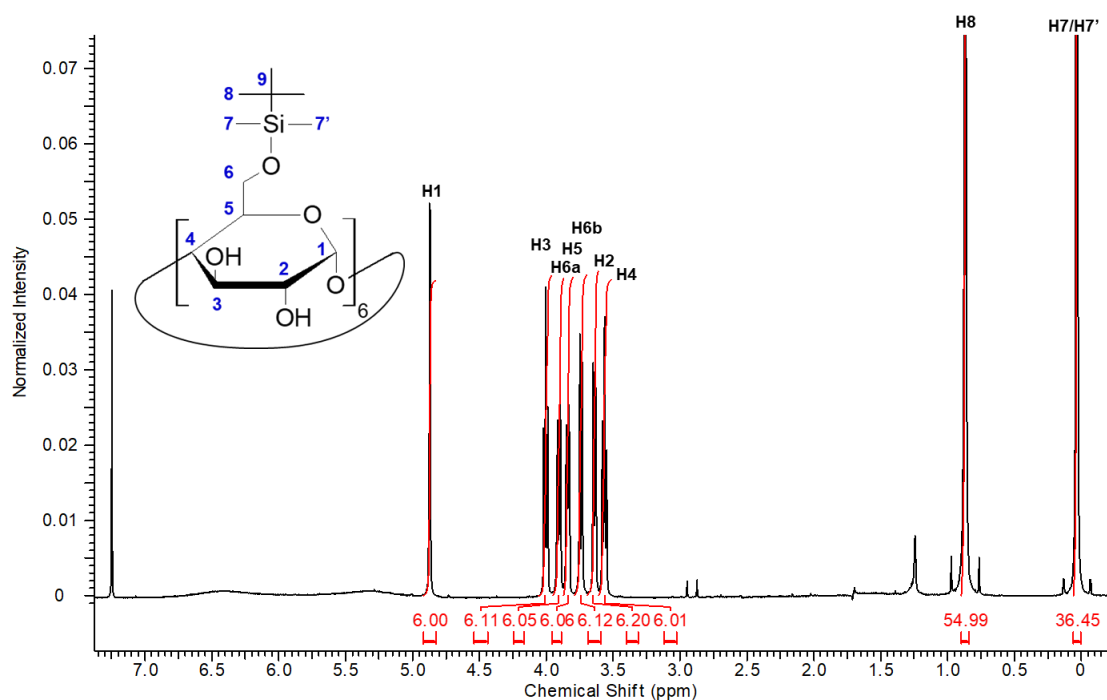


Supplementary Figure 11. Monitoring of the purification process of heptakis(6-*O*-TBDMS)- β -CD by HPLC-RID: a) reaction crude b) purified target compound c) isolated impurities.

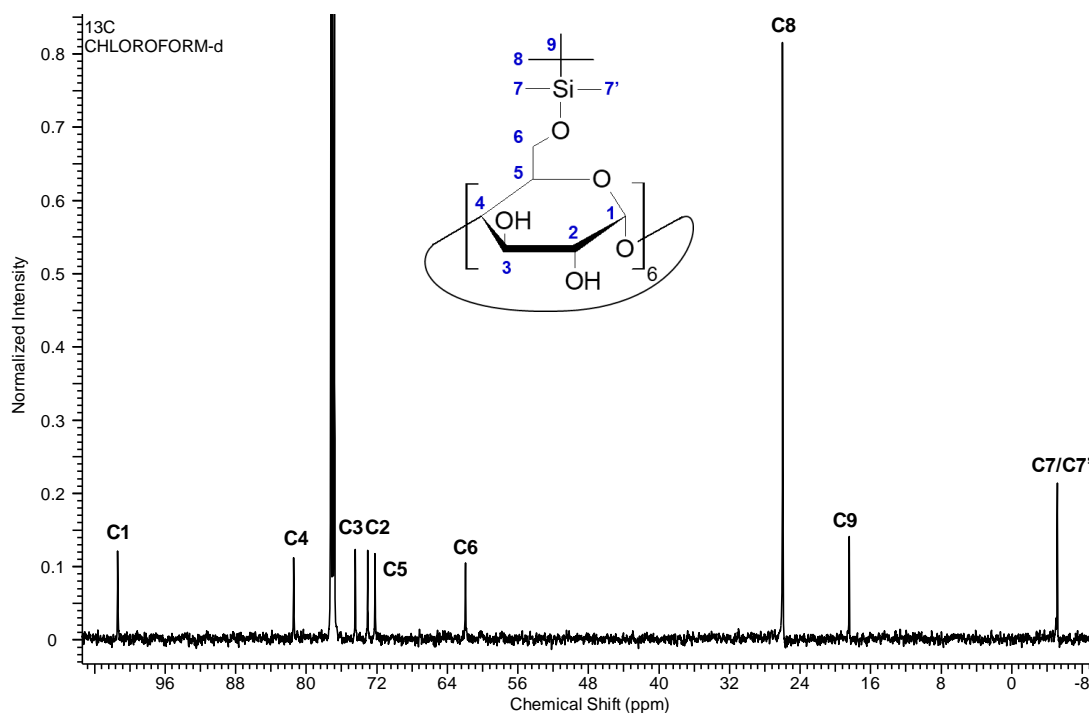


Supplementary Figure 12. Monitoring of the purification process of octakis(6-*O*-TBDMS)- γ -CD by HPLC-RID: a) reaction crude b) purified target compound c) isolated impurities.

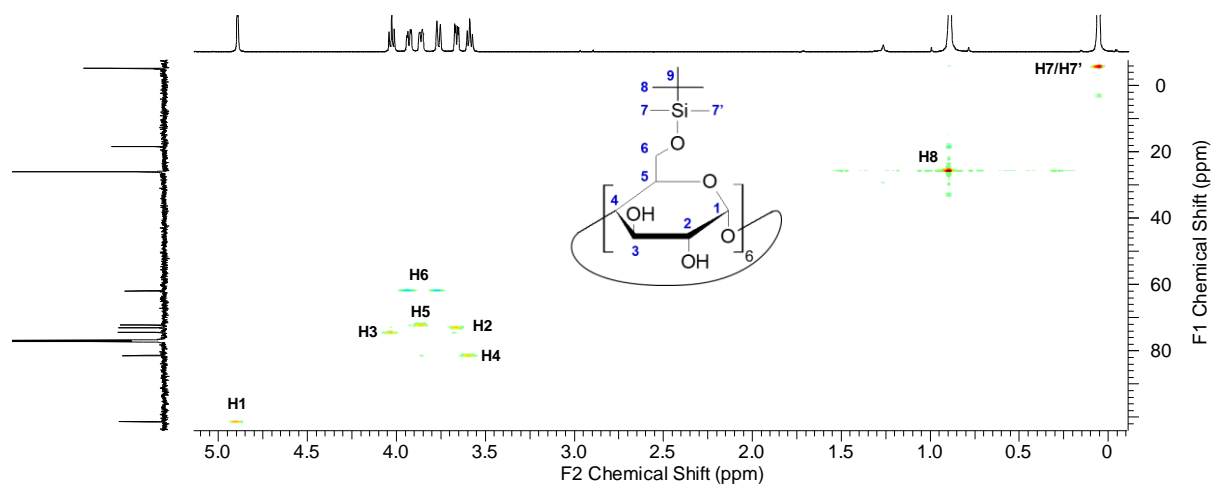
VII. NMR, MALDI and IR spectra for hexakis(6-*O*-TBDMS)- α -CD (1)



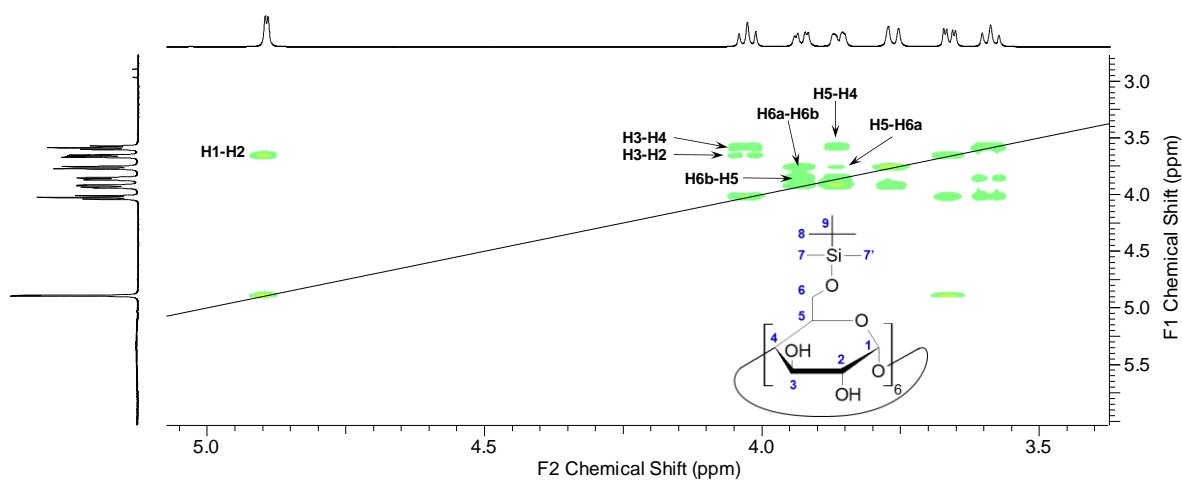
Supplementary Figure 13. ^1H spectrum of hexakis(6-*O*-TBDMS)- α -CD (1) (600 MHz, CDCl_3 , 298 K) with full assignment.



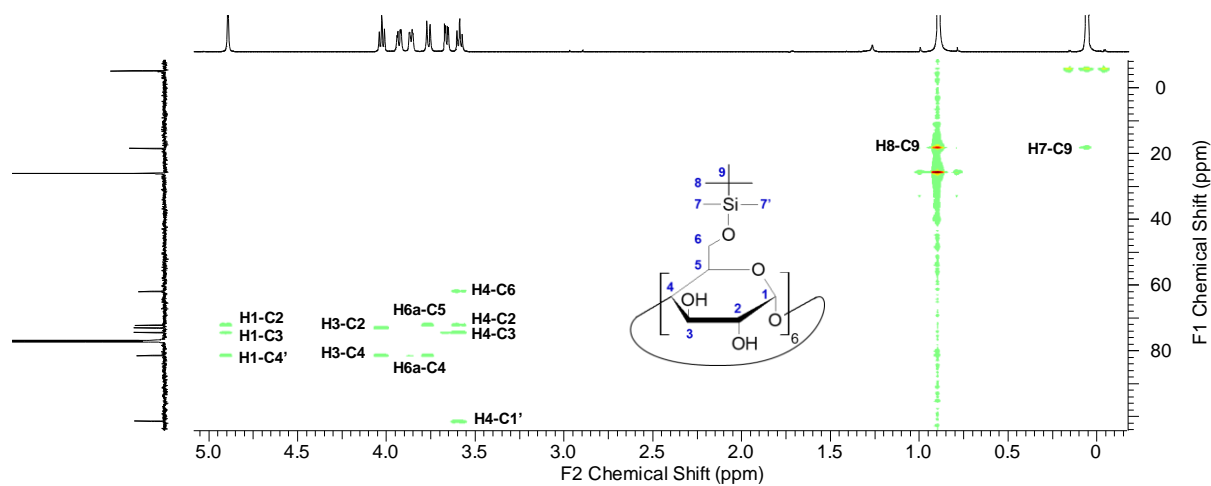
Supplementary Figure 14. ^{13}C spectrum of hexakis(6-*O*-TBDMS)- α -CD (1) (150 MHz, CDCl_3 , 298 K) with full assignment.



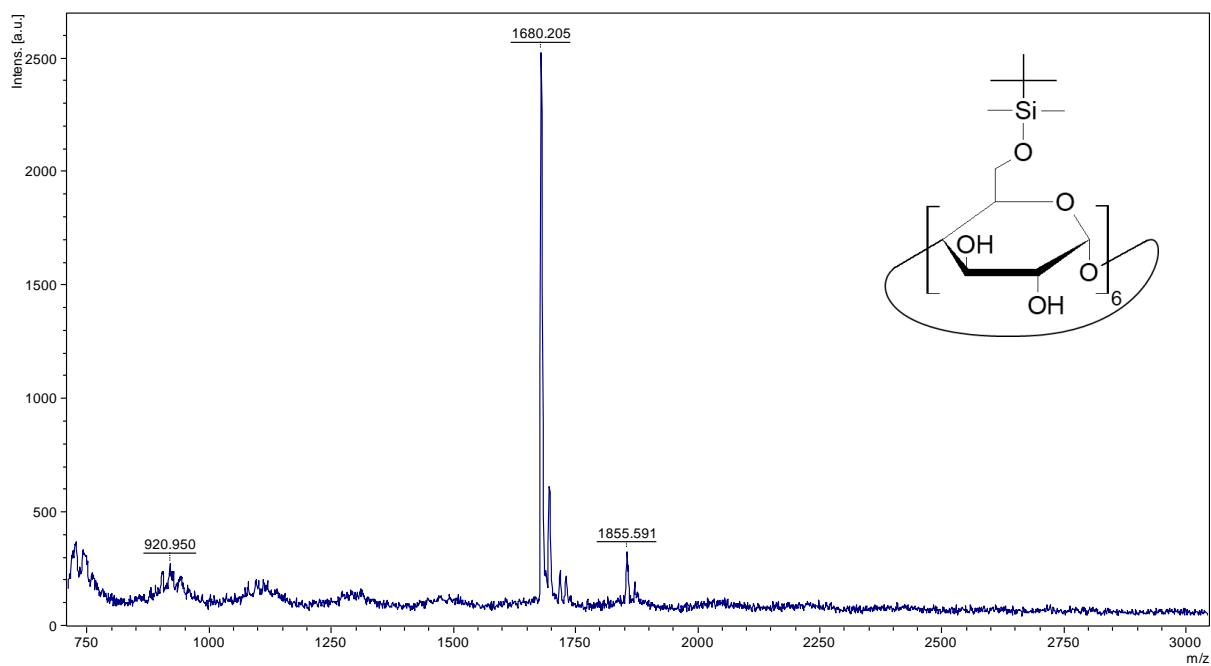
Supplementary Figure 15. DEPT-edited HSQC spectrum of hexakis(6-*O*-TBDMS)- α -CD (**1**) (600 MHz, CDCl₃, 298 K) with full assignment.



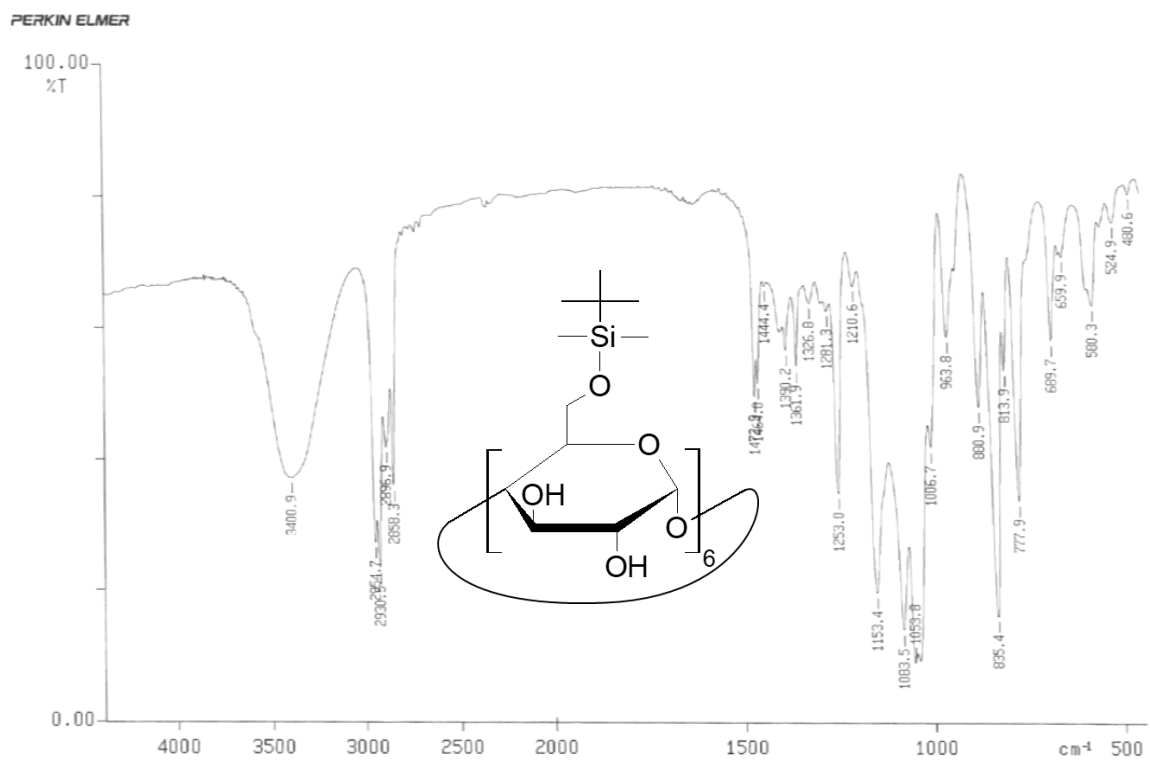
Supplementary Figure 16. COSY spectrum of hexakis(6-*O*-TBDMS)- α -CD (**1**) (600 MHz, CDCl₃, 298 K) with full assignment.



Supplementary Figure 17. HMBC spectrum of hexakis(6-*O*-TBDMS)- α -CD (**1**) (600 MHz, CDCl_3 , 298 K) with full assignment.

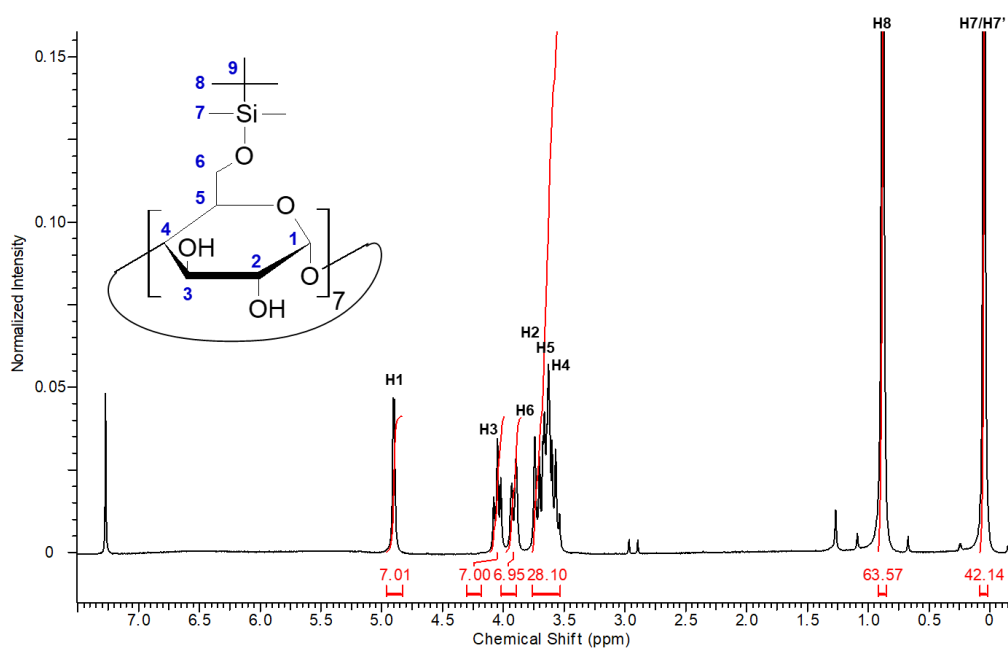


Supplementary Figure 18. MALDI spectrum of hexakis(6-*O*-TBDMS)- α -CD (**1**) (DHB as matrix).

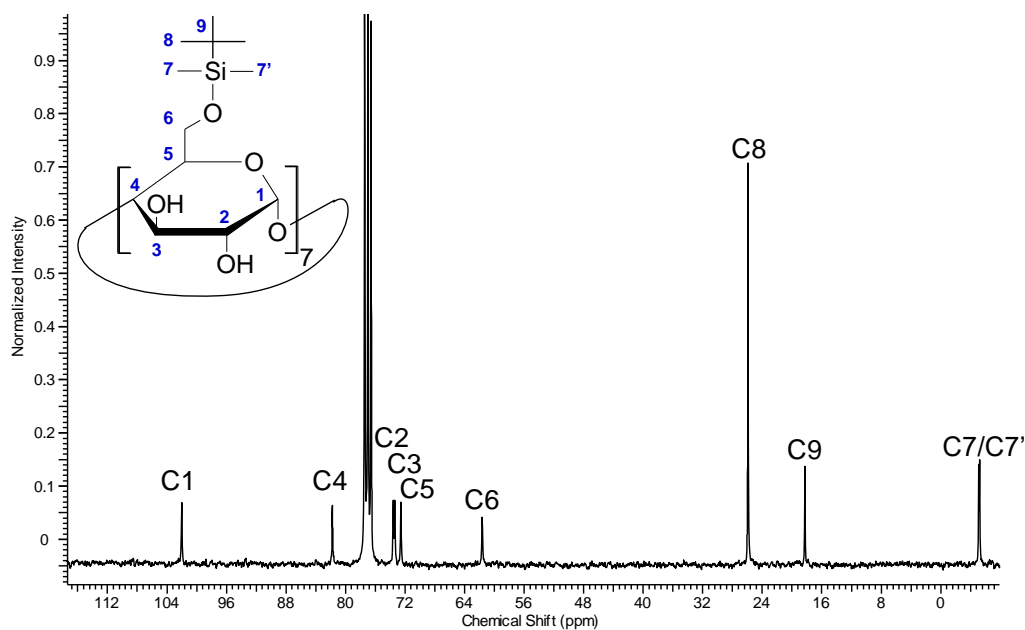


Supplementary Figure 19. IR spectrum of hexakis(6-*O*-TBDMS)- α -CD (**1**) (KBr disk).

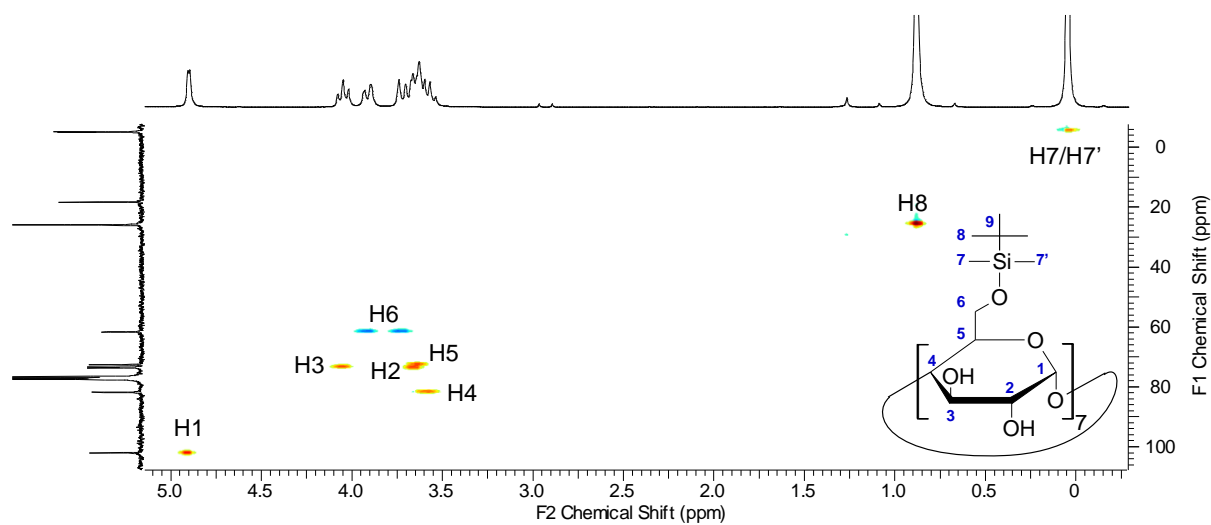
VIII. NMR, MALDI and IR spectra for heptakis(6-*O*-TBDMS)- β -CD (2)



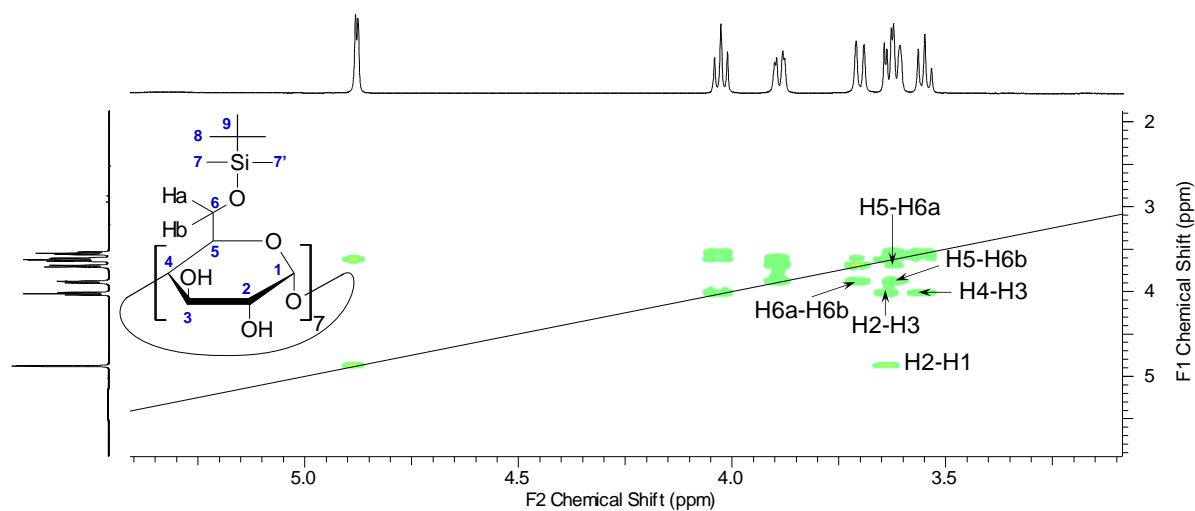
Supplementary Figure 20. ^1H spectrum of heptakis(6-*O*-TBDMS)- β -CD (2) (600 MHz, CDCl_3 , 298 K) with full assignment.



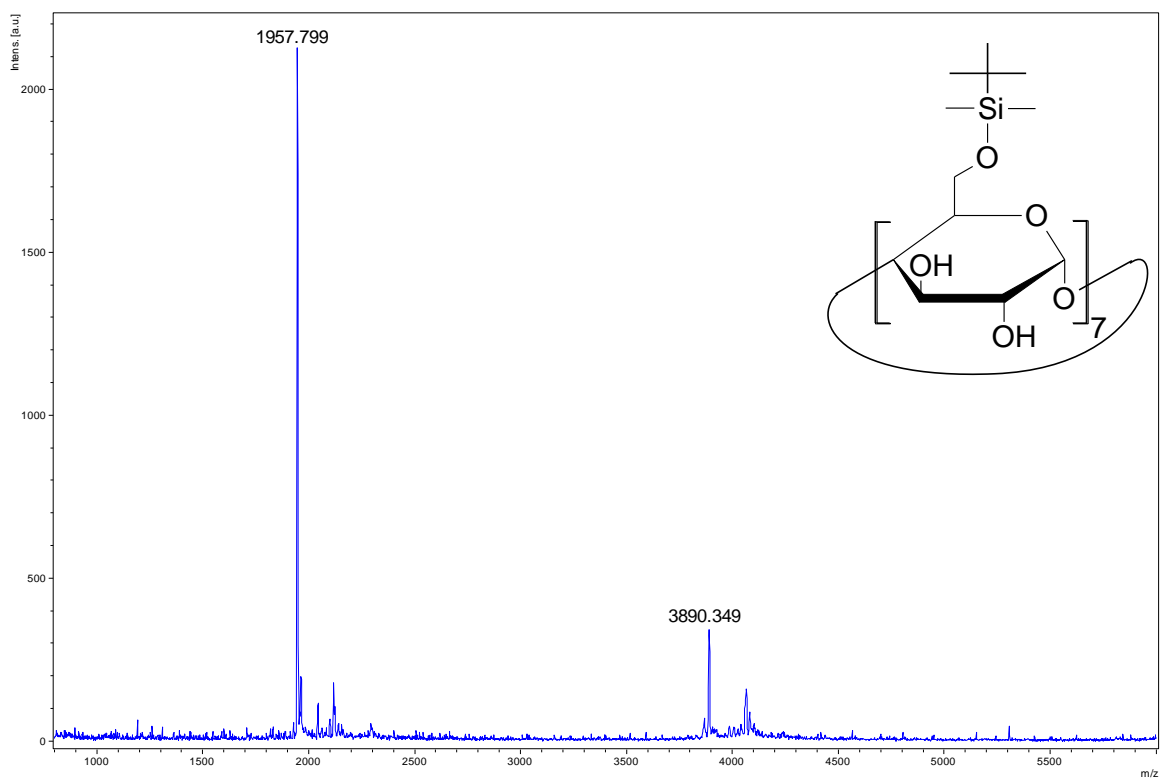
Supplementary Figure 21. ^{13}C spectrum of heptakis(6-*O*-TBDMS)- β -CD (2) (150 MHz, CDCl_3 , 298 K) with full assignment.



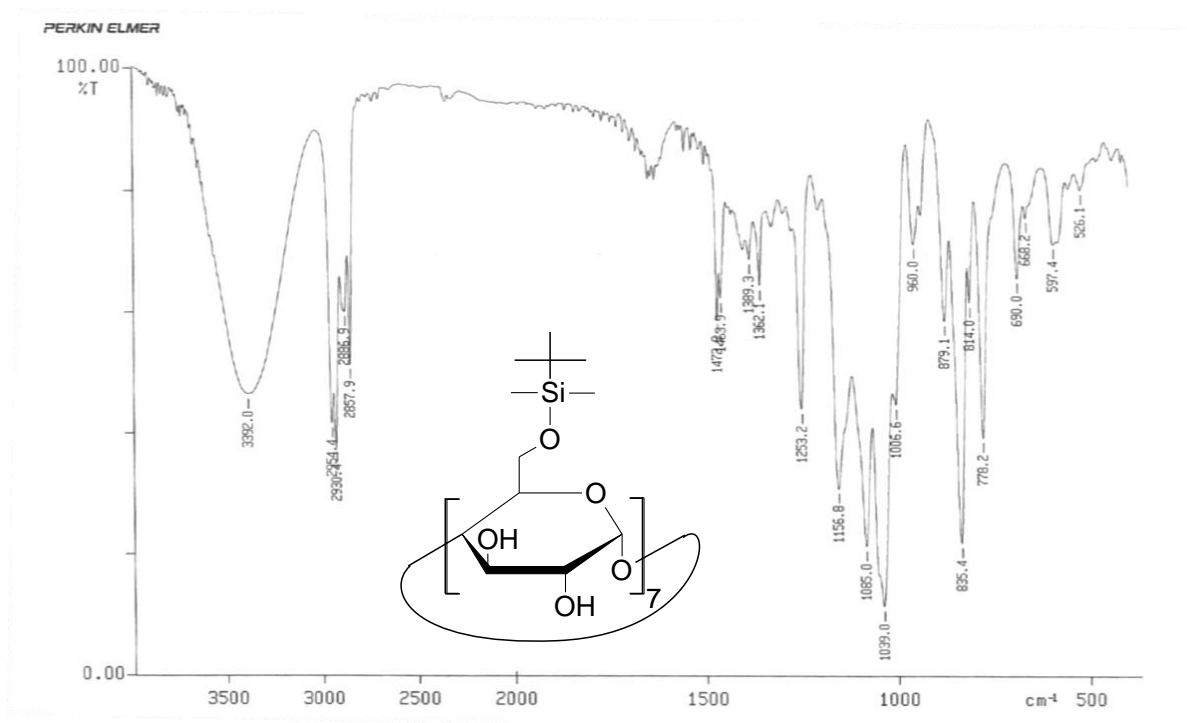
Supplementary Figure 22. DEPT-edited HSQC spectrum of heptakis(6-*O*-TBDMS)- β -CD (2) (600 MHz, CDCl_3 , 298 K) with full assignment.



Supplementary Figure 23. COSY spectrum of heptakis(6-*O*-TBDMS)- β -CD (2) (600 MHz, CDCl_3 , 298 K) with full assignment.

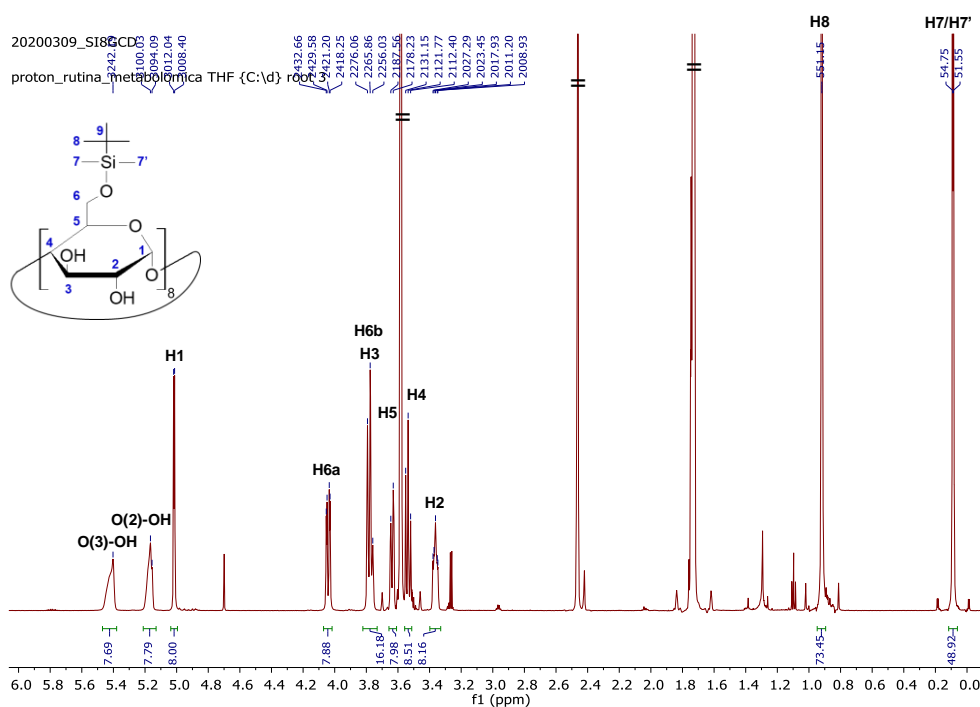


Supplementary Figure 24. MALDI spectrum of heptakis(6-*O*-TBDMS)-β-CD (**2**) (DHB as matrix).

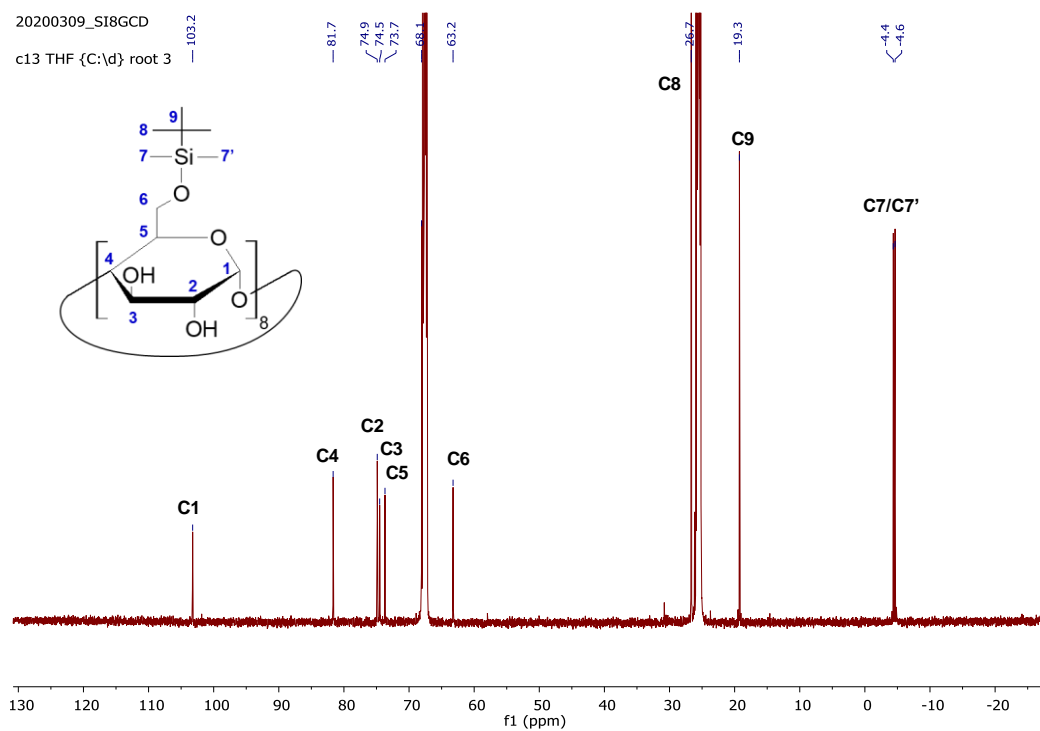


Supplementary Figure 25. IR spectrum of heptakis(6-*O*-TBDMS)-β-CD (**2**) (KBr disk).

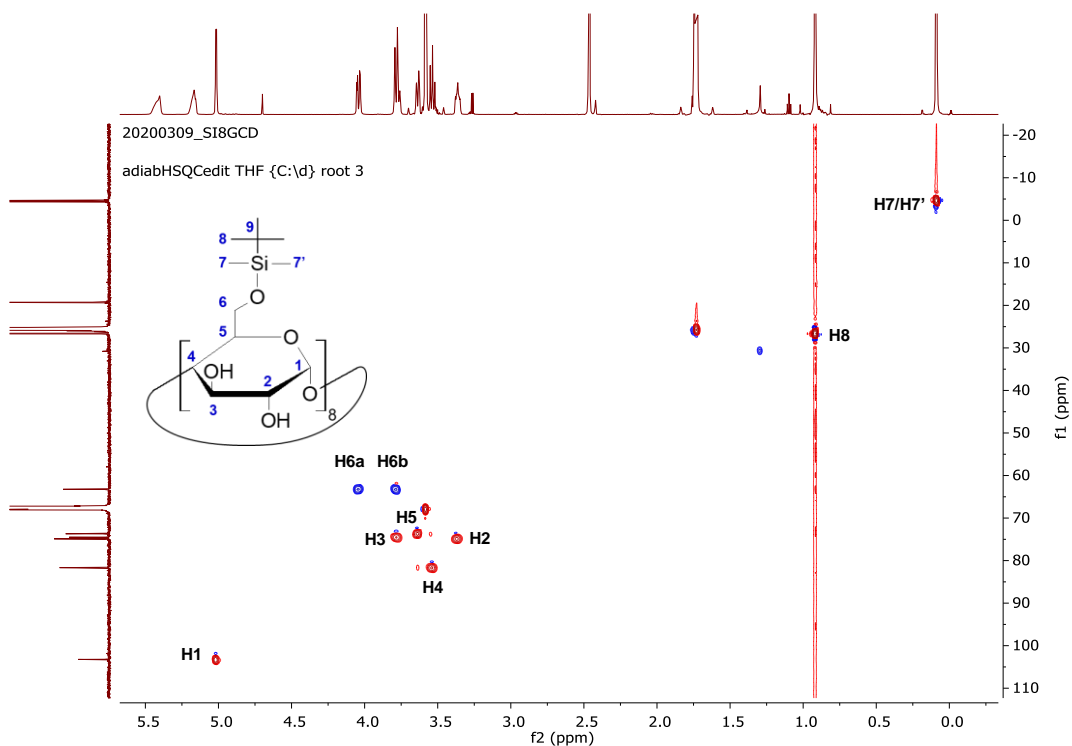
IX. NMR, MALDI and IR spectra for octakis(6-*O*-TBDMS)- γ -CD (3)



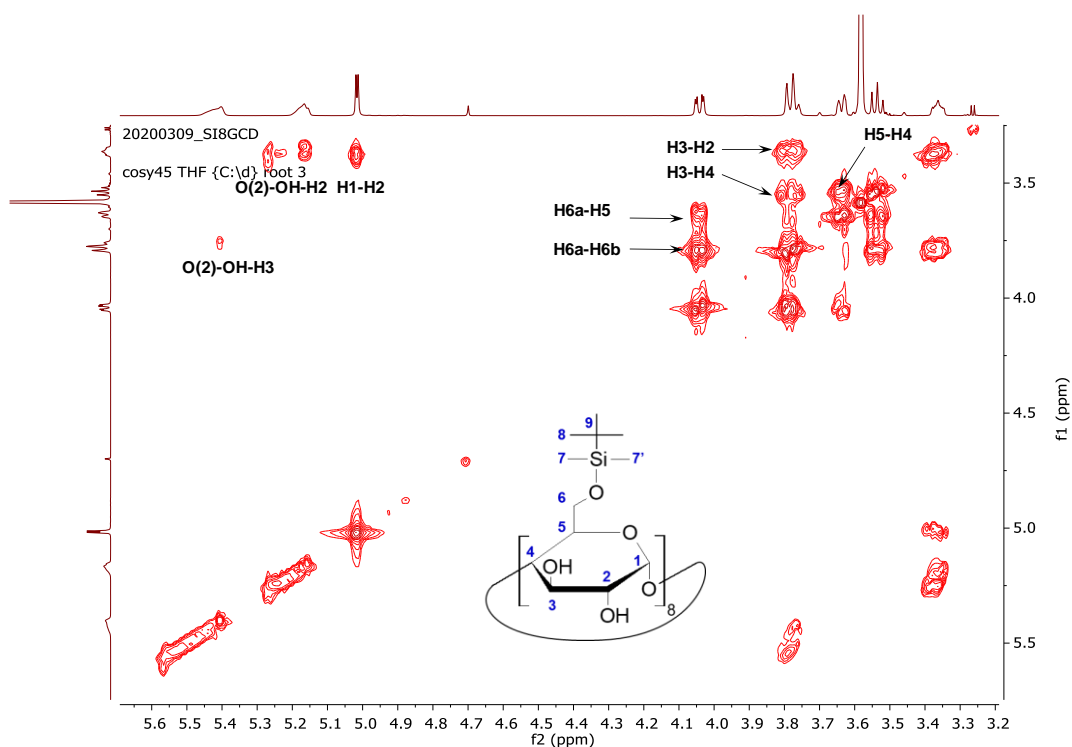
Supplementary Figure 26. ^1H spectrum of octakis(6-*O*-TBDMS)- γ -CD (3) (600 MHz, THF- d_8 , 298 K) with full assignment.



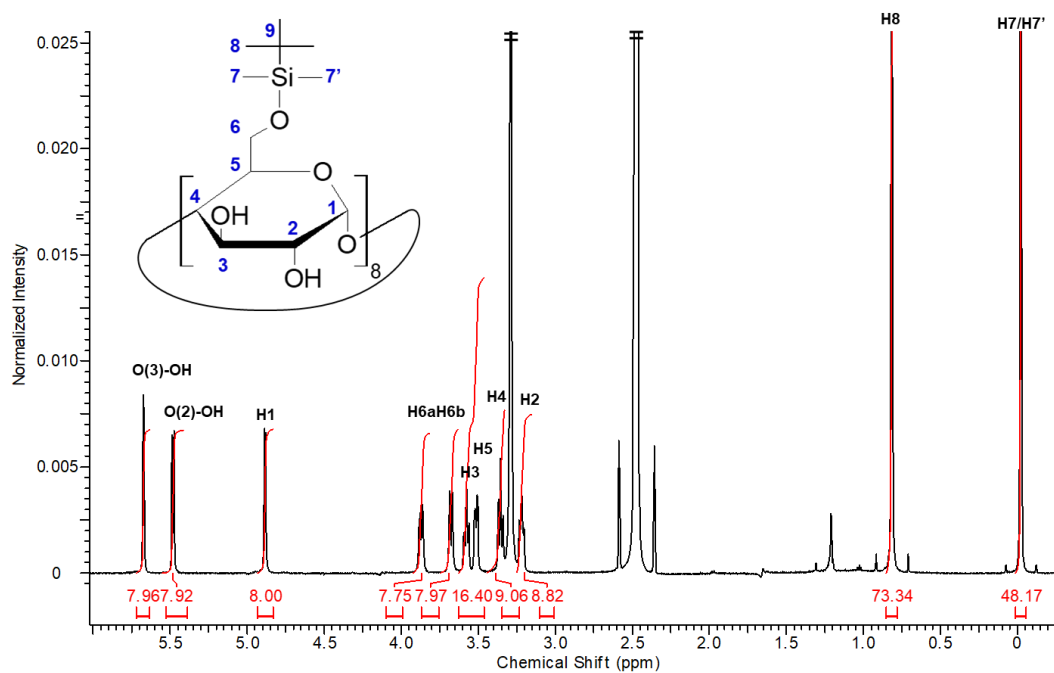
Supplementary Figure 27. ^{13}C spectrum of octakis(6-*O*-TBDMS)- γ -CD (3) (150 MHz, THF- d_8 , 298 K) with full assignment.



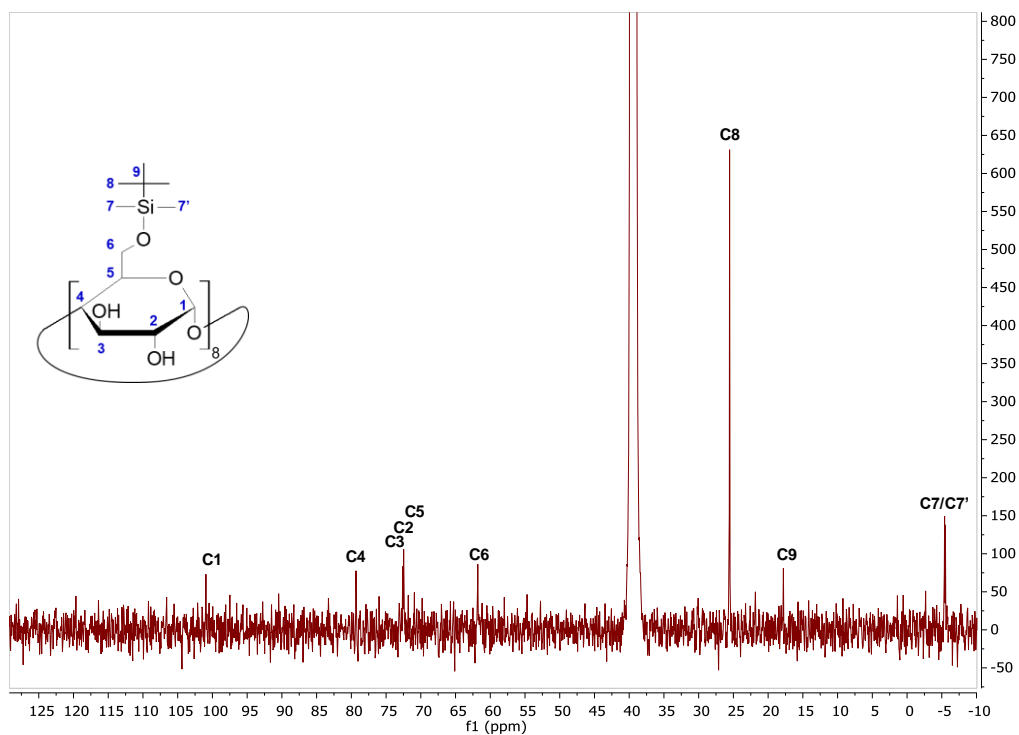
Supplementary Figure 28. DEPT-edited HSQC spectrum of octakis(6-*O*-TBDMS)- γ -CD (**3**) (600 MHz, THF-*d*₈, 298 K) with full assignment.



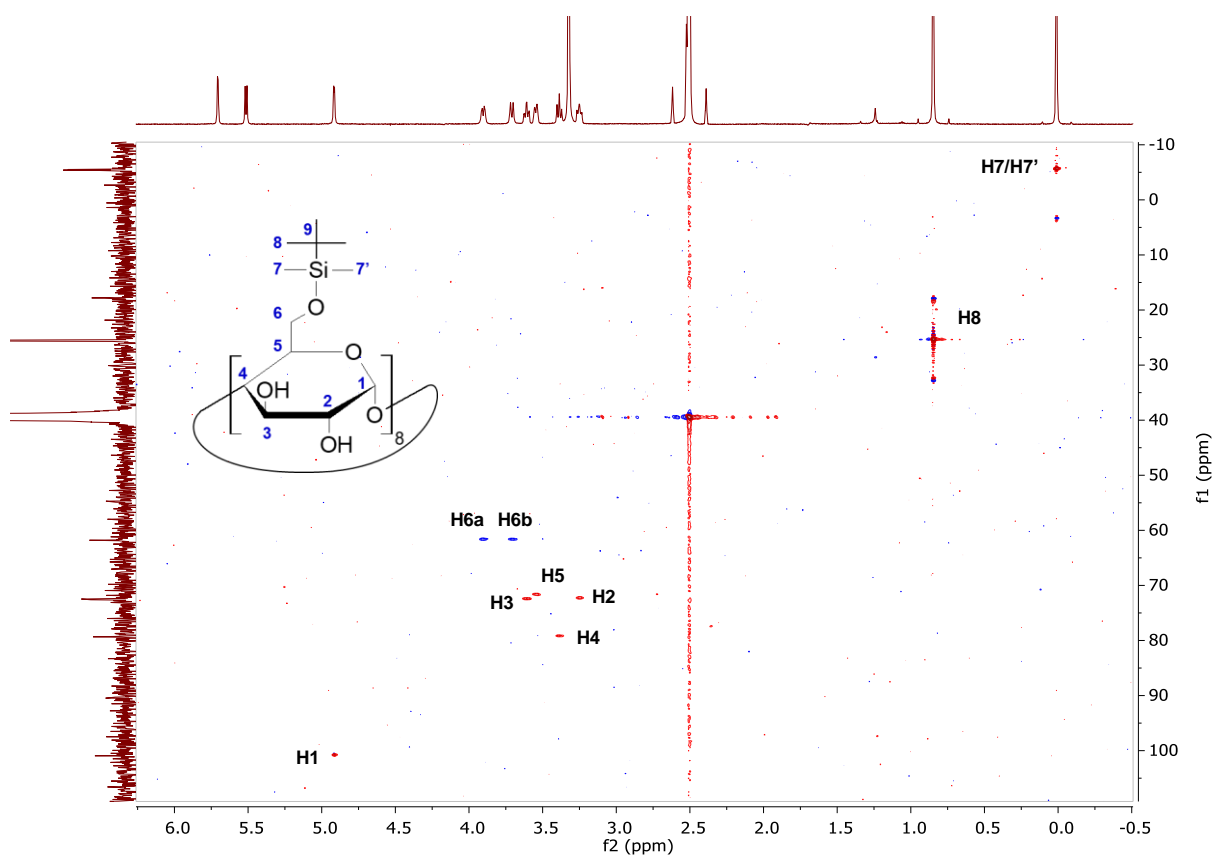
Supplementary Figure 29. COSY spectrum of octakis(6-*O*-TBDMS)- γ -CD (**3**) (600 MHz, THF-*d*₈, 298 K) with full assignment.



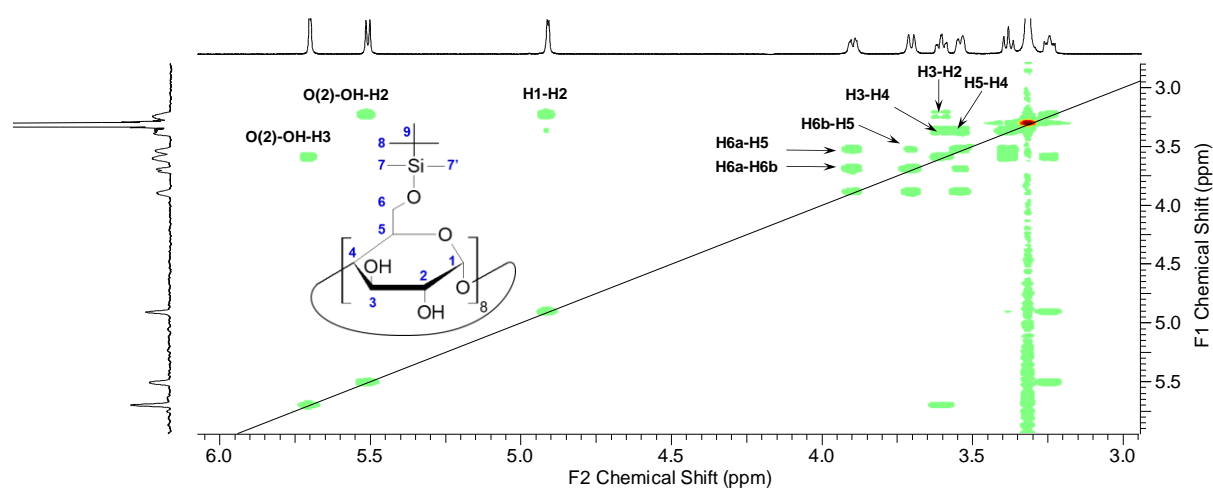
Supplementary Figure 30. ^1H spectrum of octakis(6-*O*-TBDMS)- γ -CD (**3**) (600 MHz, $\text{DMSO-}d_6$, 298 K) with full assignment.



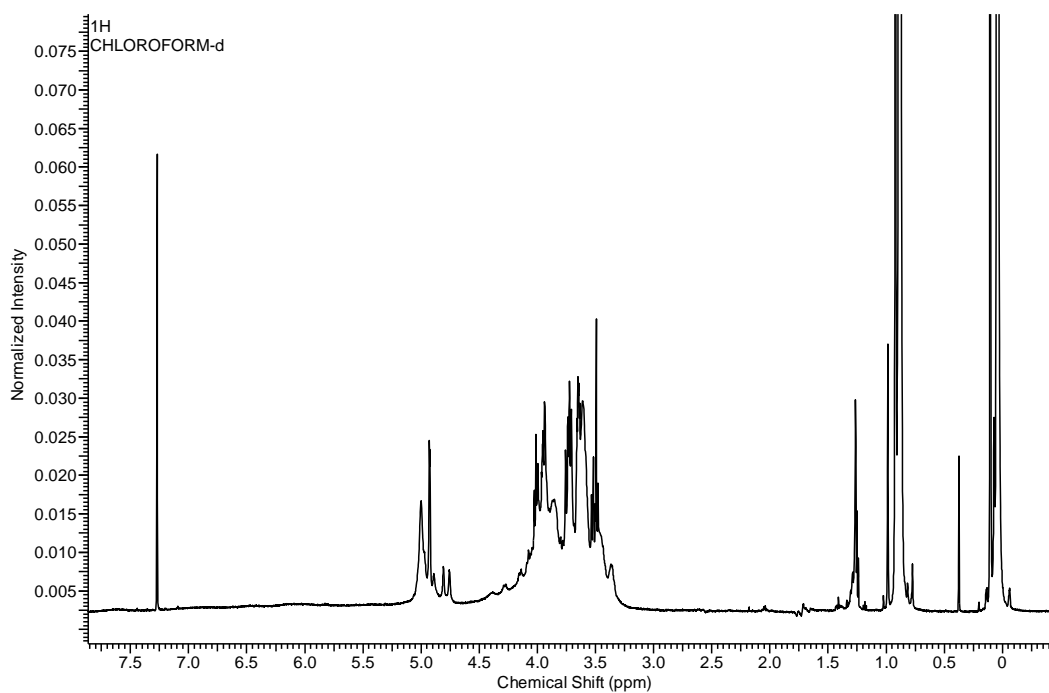
Supplementary Figure 31. ^{13}C spectrum of octakis(6-*O*-TBDMS)- γ -CD (**3**) (150 MHz, $\text{DMSO-}d_6$, 298 K) with full assignment.



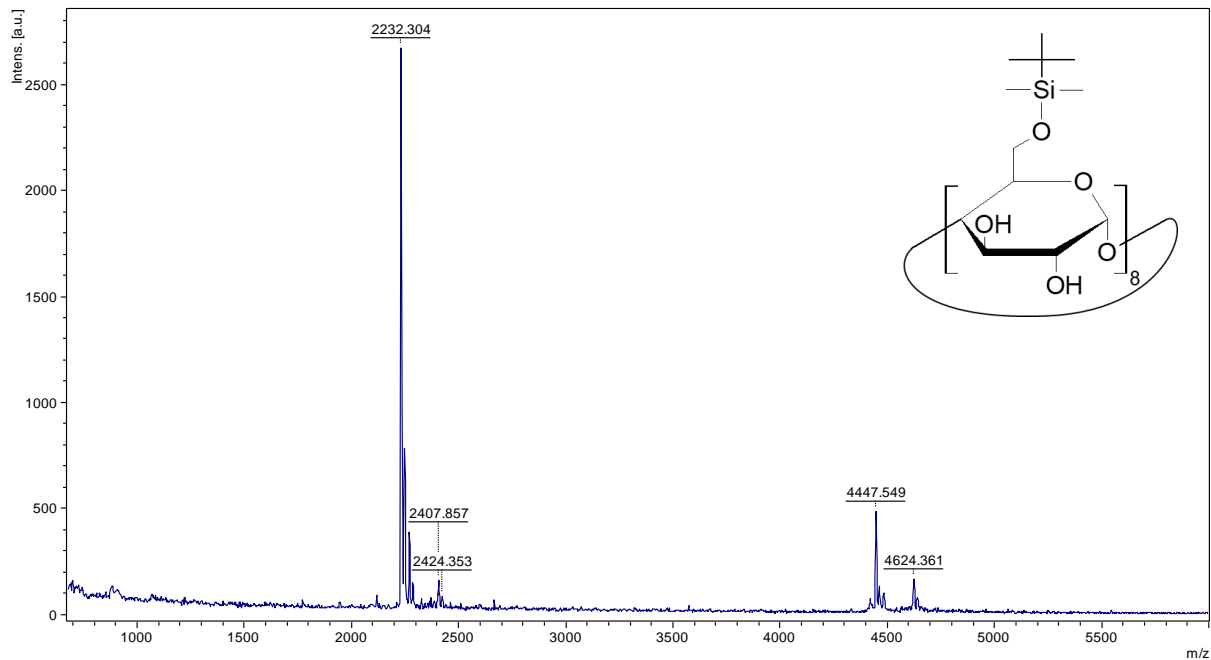
Supplementary Figure 32. DEPT-edited HSQC spectrum of octakis(6-*O*-TBDMS)- γ -CD (**3**) (600 MHz, DMSO- d_6 , 298 K) with full assignment.



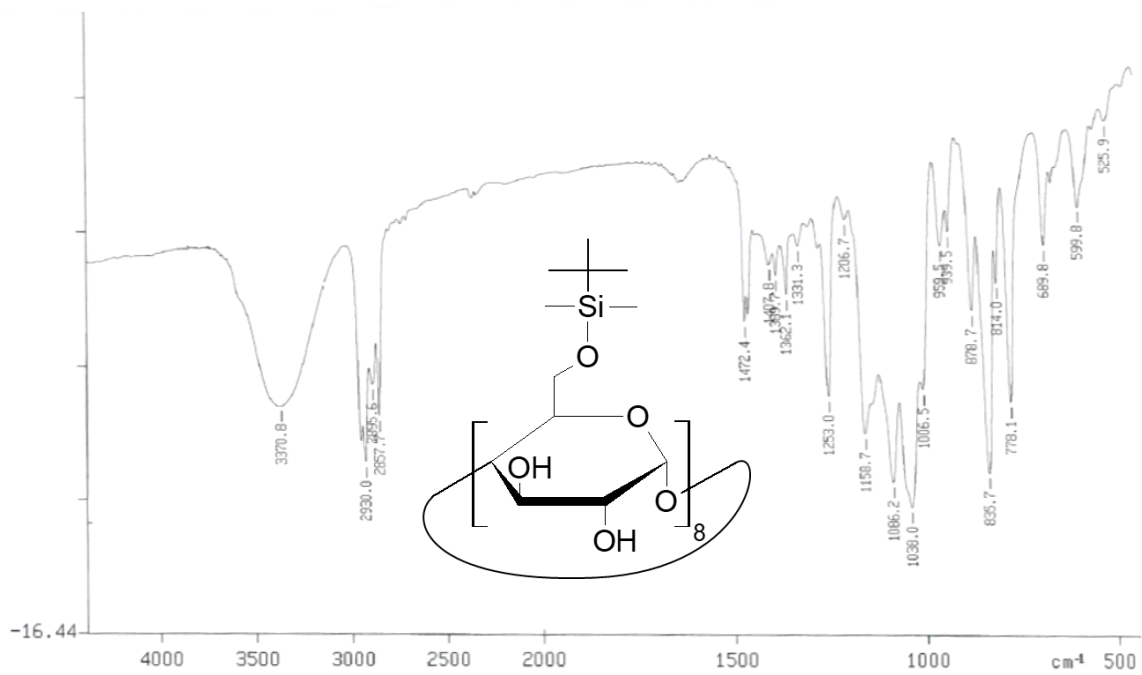
Supplementary Figure 33. COSY spectrum of octakis(6-*O*-TBDMS)- γ -CD (**3**) (600 MHz, DMSO- d_6 , 298 K) with full assignment.



Supplementary Figure 34. ^1H spectrum of heptakis(6-*O*-TBDMS)- γ -CD (**3**) (600 MHz, CDCl_3 , 298 K).

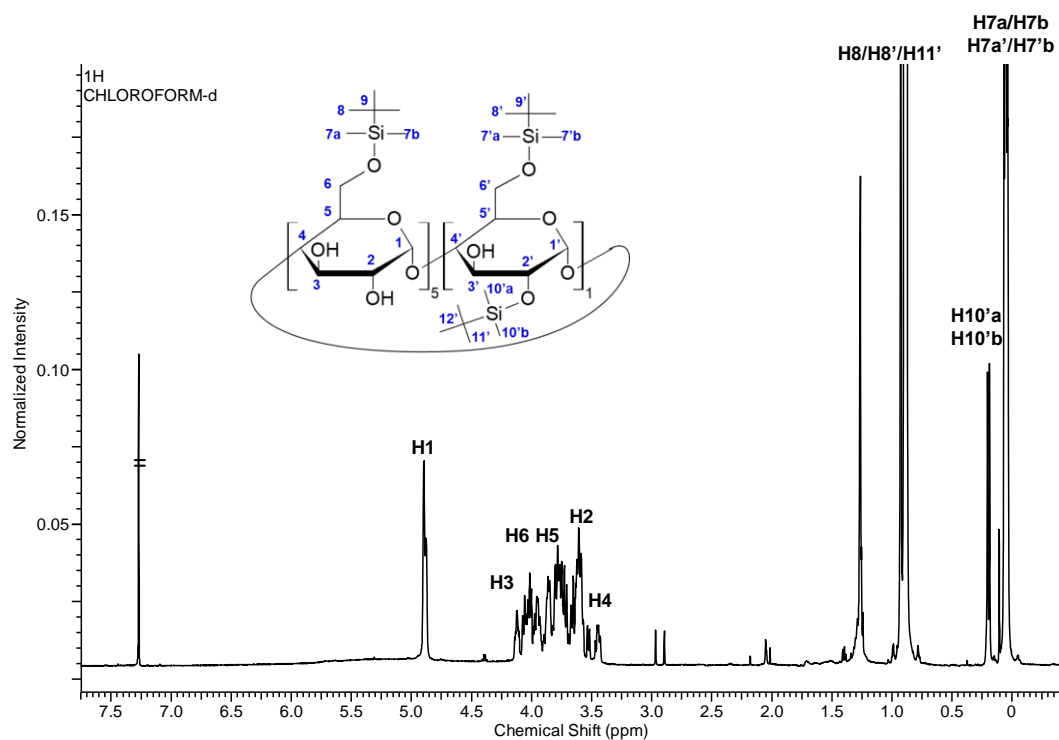


Supplementary Figure 35. MALDI spectrum of octakis(6-*O*-TBDMS)- γ -CD (**3**) (DHB as matrix).

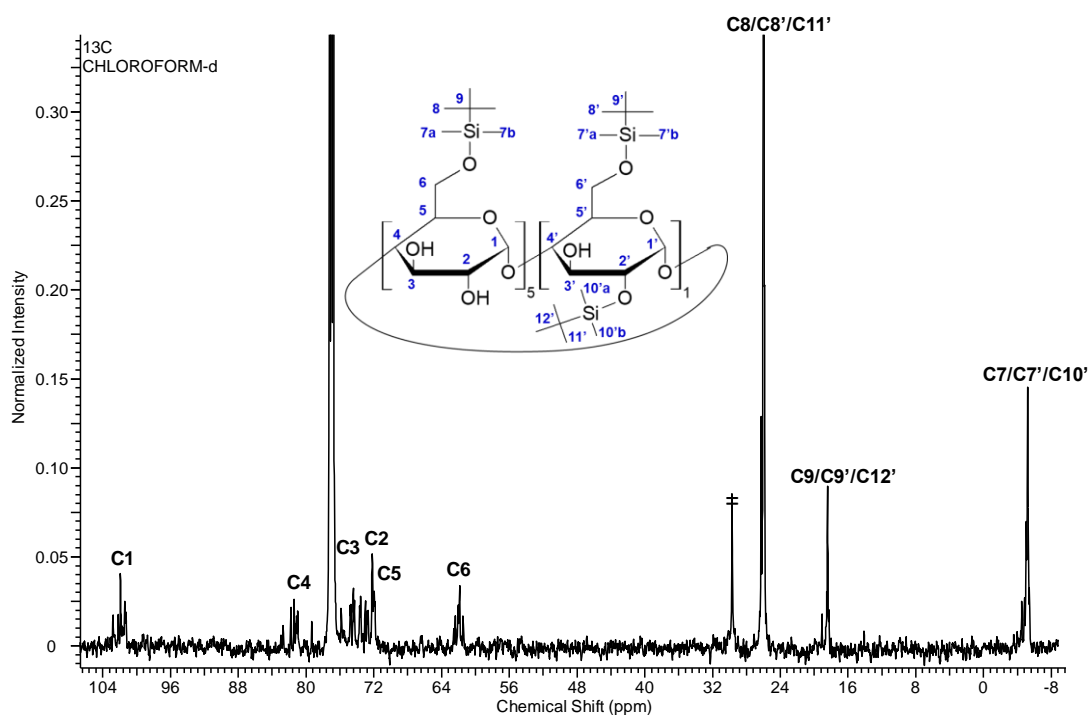


Supplementary Figure 36. IR spectrum of octakis(6-O-TBDMS)- γ -CD (3) (KBr disk).

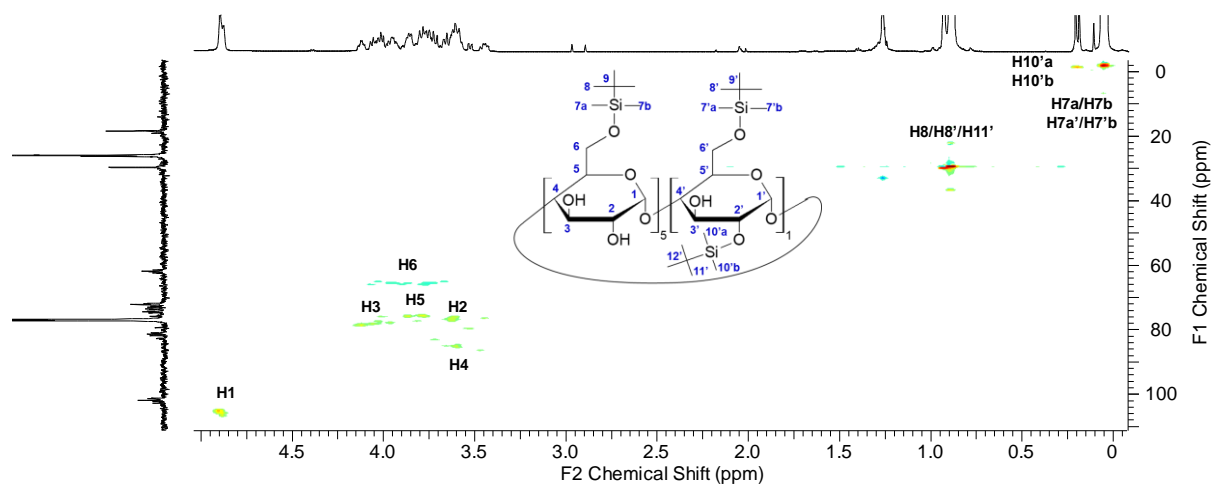
X. NMR, MALDI and IR spectra for oversilylated α -CD derivative



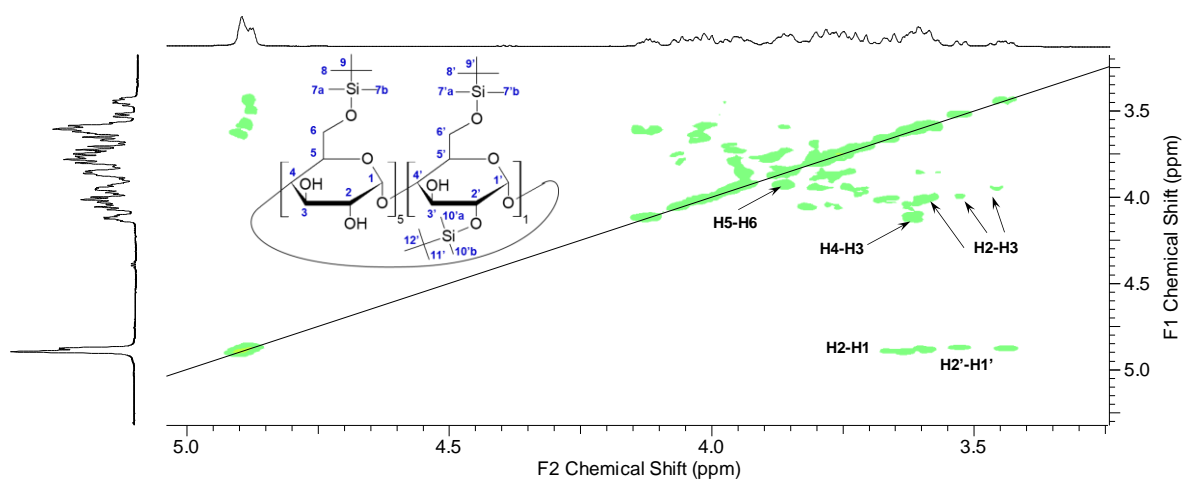
Supplementary Figure 37. ¹H spectrum of oversilylated α -CD derivative (600 MHz, CDCl₃, 298 K) with partial assignment. Depicted structure is tentative.



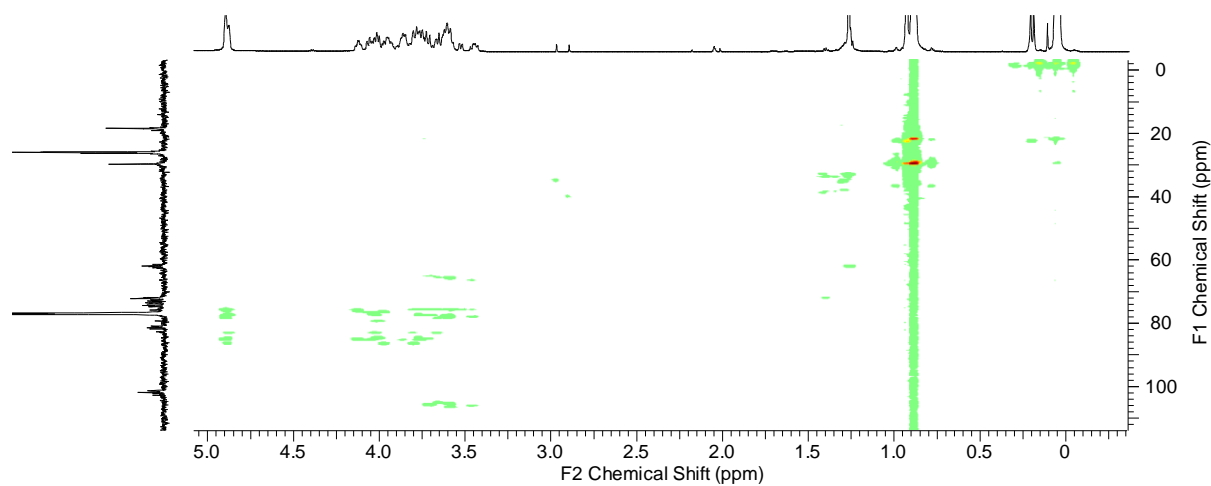
Supplementary Figure 38. ¹³C spectrum of oversilylated α -CD derivative (150 MHz, CDCl₃, 298 K) with partial assignment. Depicted structure is tentative.



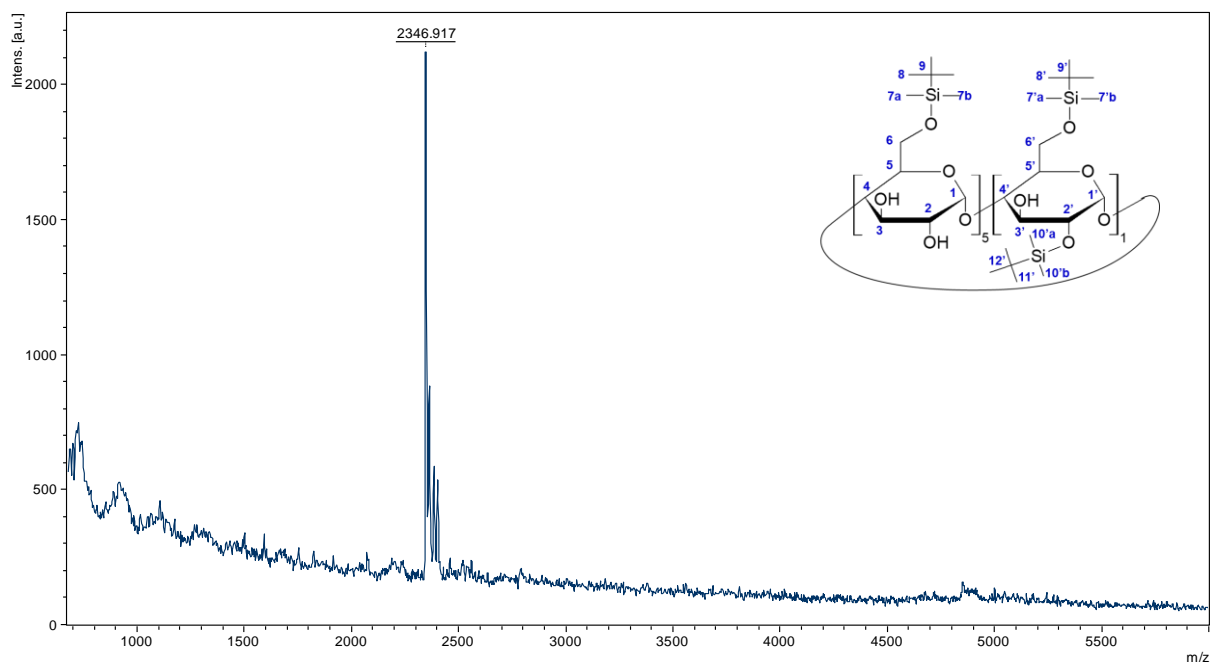
Supplementary Figure 39. DEPT-edited HSQC spectrum of oversilylated α -CD derivative (600 MHz, CDCl_3 , 298 K) with partial assignment. Depicted structure is tentative.



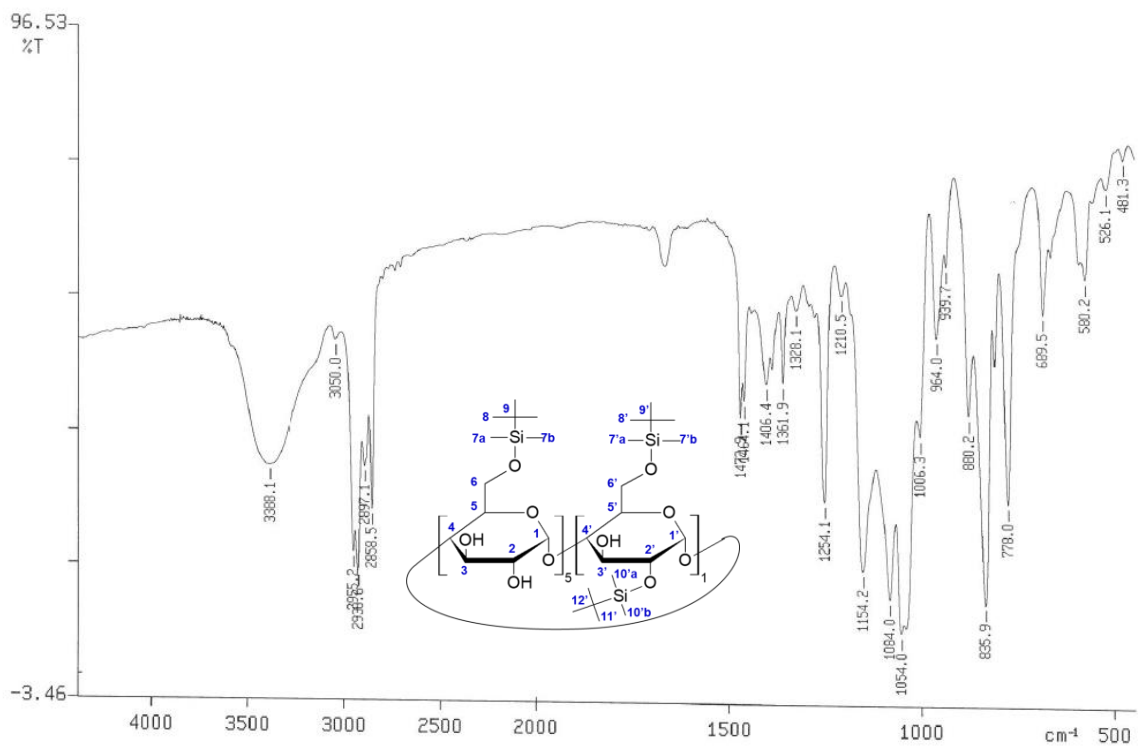
Supplementary Figure 40. COSY spectrum of oversilylated α -CD derivative (600 MHz, CDCl_3 , 298 K) with partial assignment. Depicted structure is tentative.



Supplementary Figure 41. HMBC spectrum of oversilylated α -CD derivative (600 MHz, CDCl_3 , 298 K). Depicted structure is tentative.

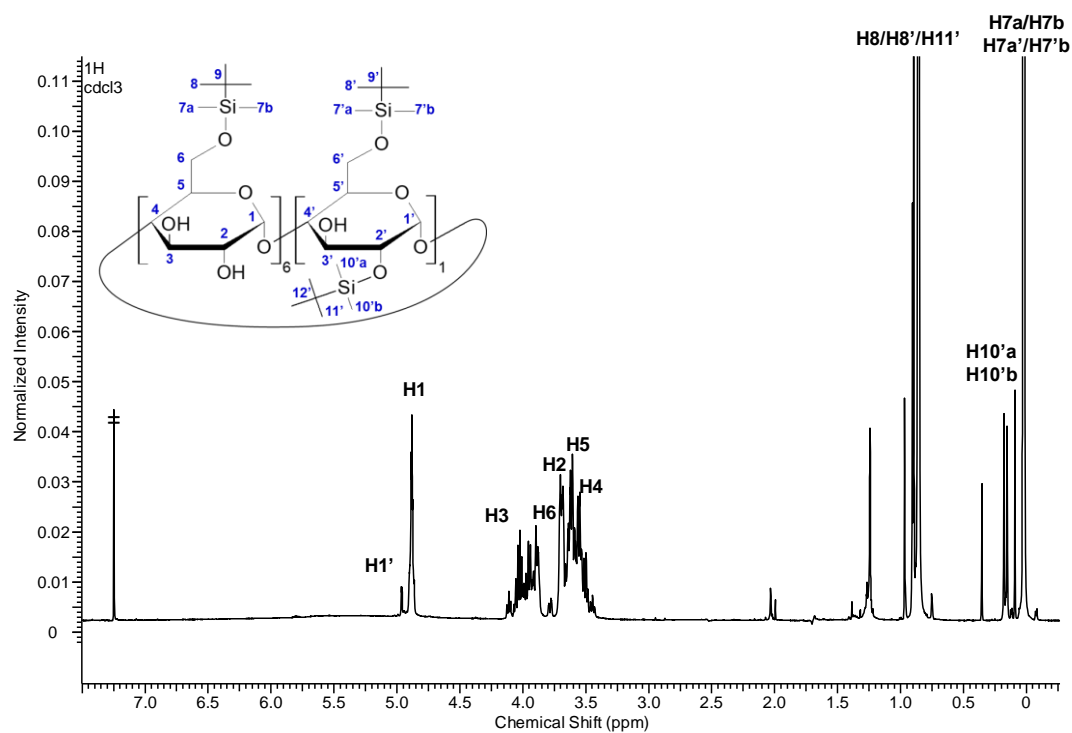


Supplementary Figure 42. MALDI spectrum of oversilylated α -CD derivative (DHB as matrix). Depicted structure is tentative.

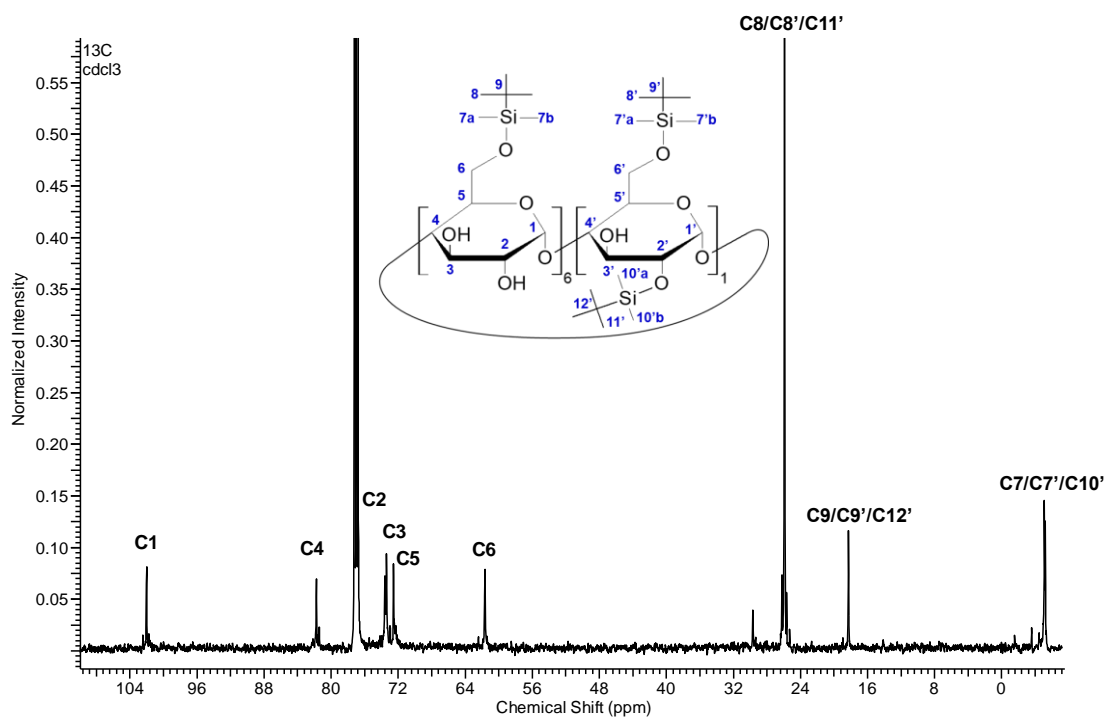


Supplementary Figure 43. IR spectrum of oversilylated α -CD derivative (KBr disk). Depicted structure is tentative.

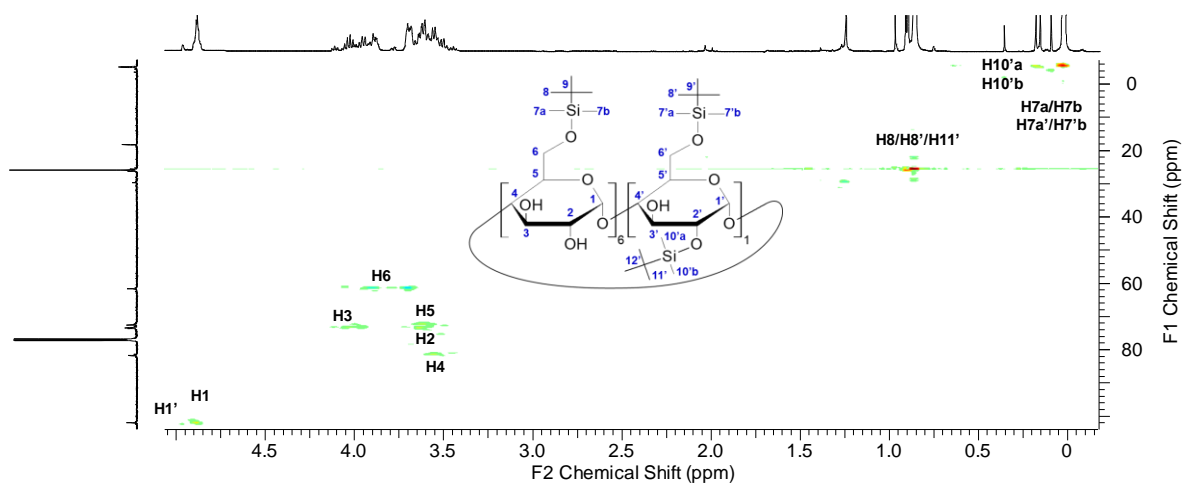
XI. NMR, MALDI and IR spectra for oversilylated β -CD derivative



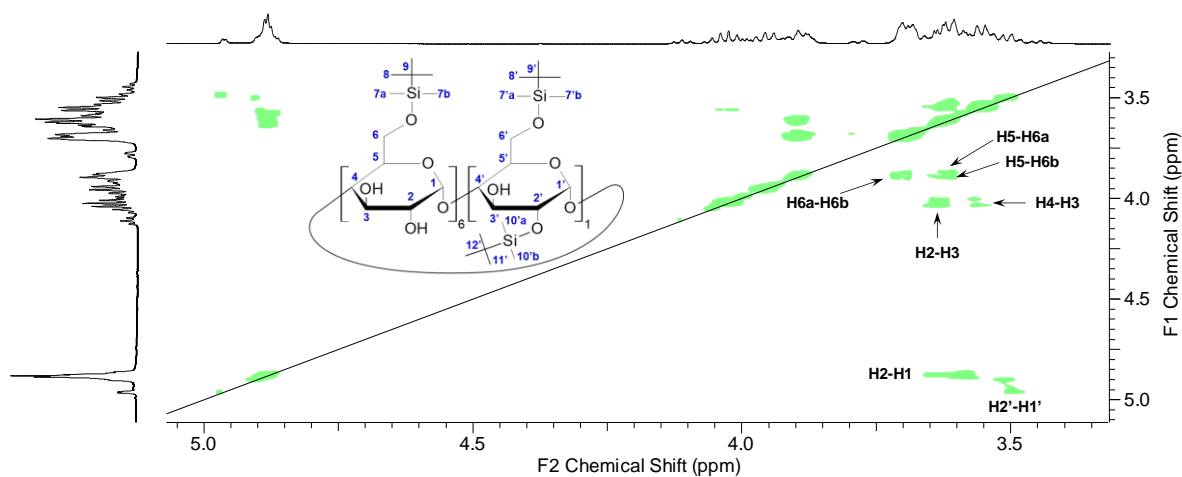
Supplementary Figure 44. ^1H spectrum of oversilylated β -CD derivative (600 MHz, CDCl_3 , 298 K) with partial assignment. Depicted structure is tentative.



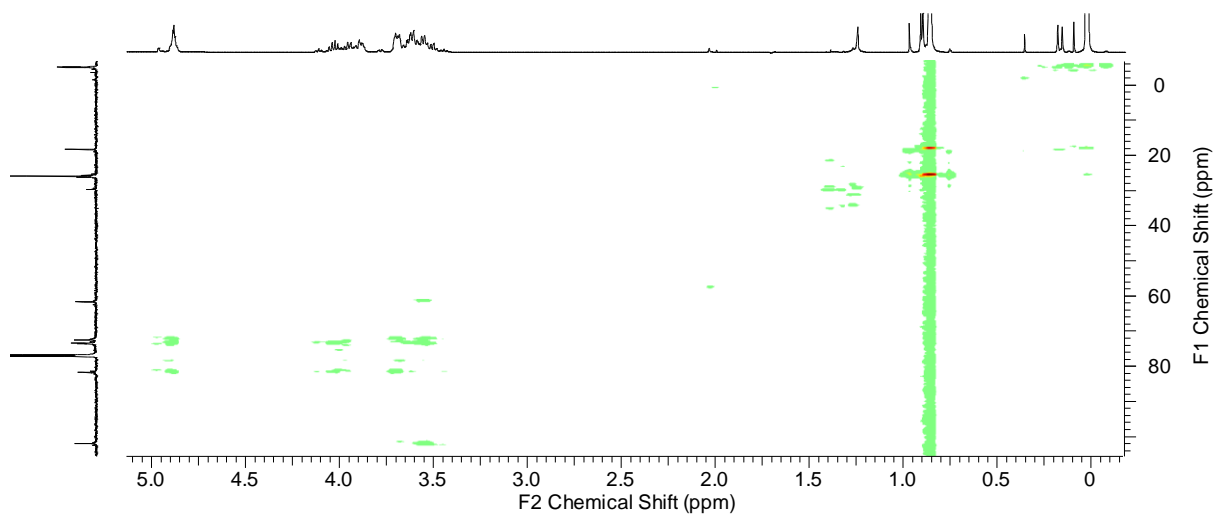
Supplementary Figure 45. ^{13}C spectrum of oversilylated β -CD derivative (150 MHz, CDCl_3 , 298 K) with partial assignment. Depicted structure is tentative.



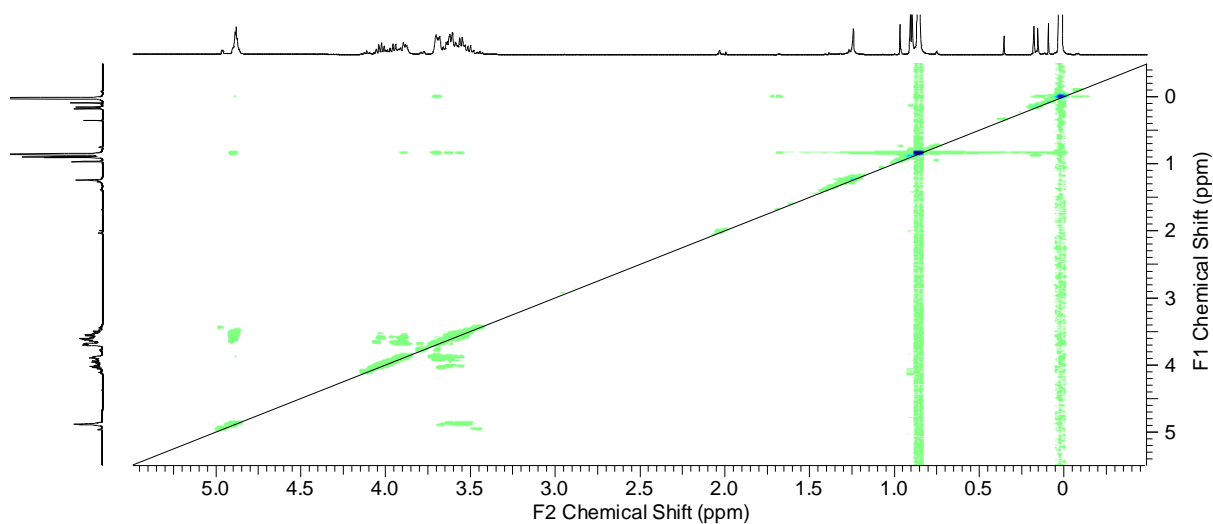
Supplementary Figure 46. DEPT-edited HSQC spectrum of oversilylated β -CD derivative (600 MHz, CDCl_3 , 298 K) with partial assignment. Depicted structure is tentative.



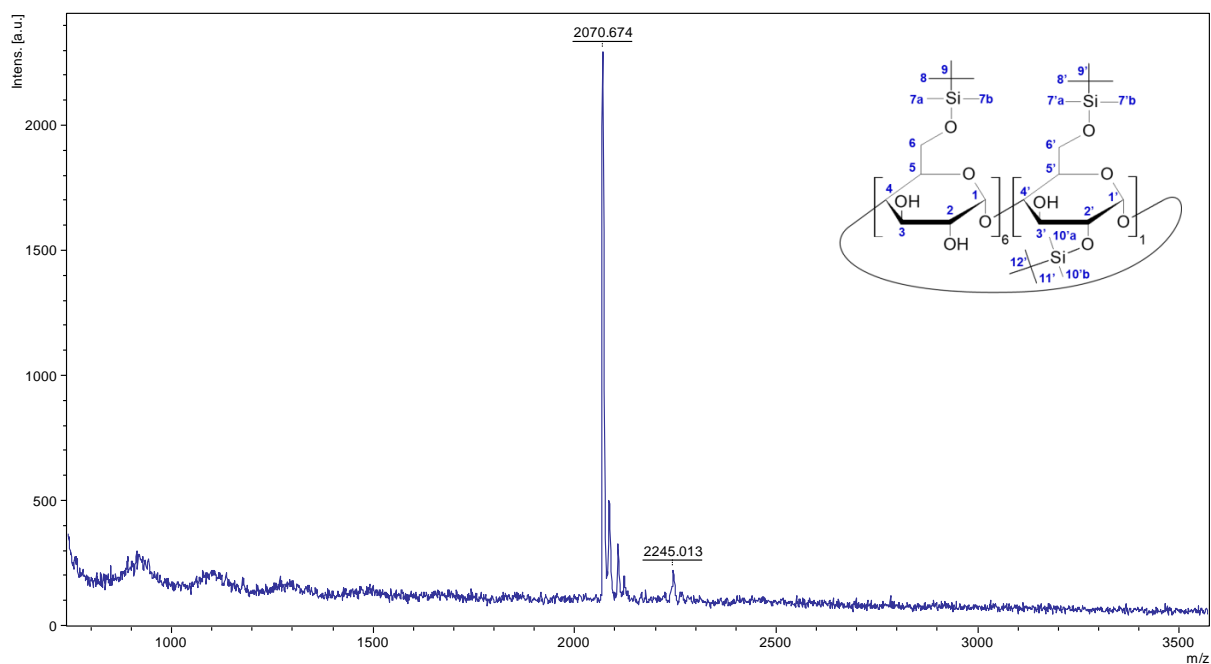
Supplementary Figure 47. COSY spectrum of oversilylated β -CD derivative (600 MHz, CDCl_3 , 298 K) with partial assignment. Depicted structure is tentative.



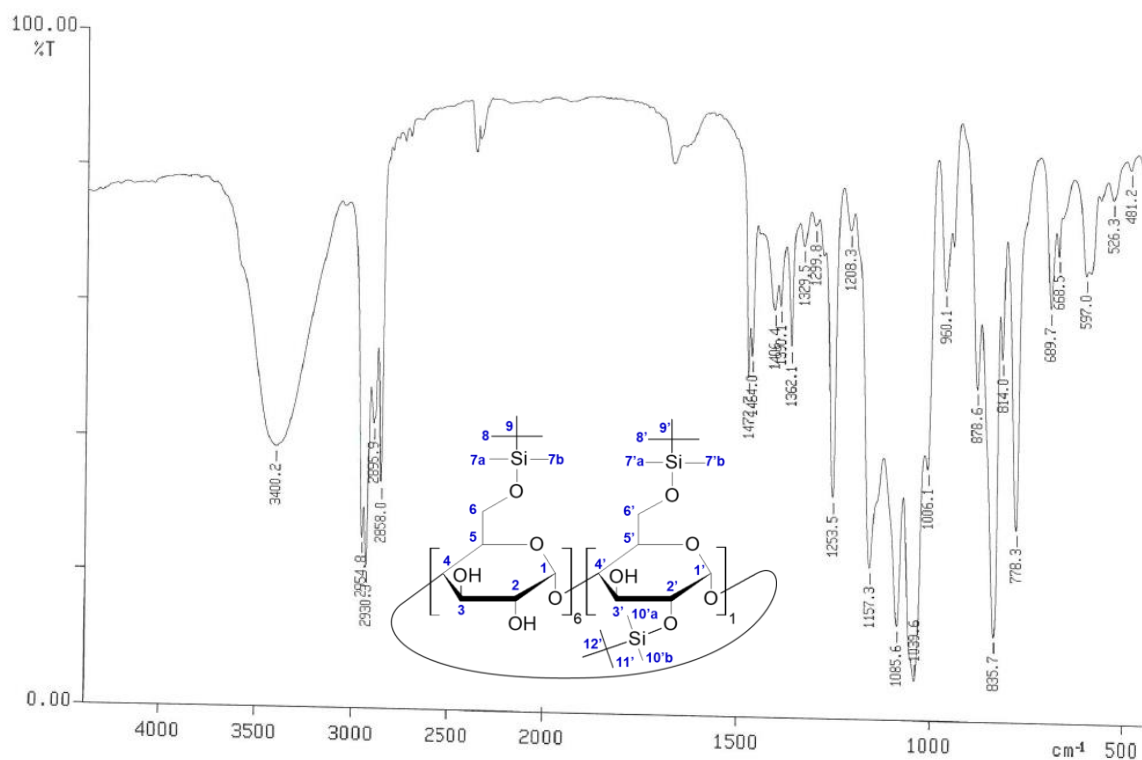
Supplementary Figure 48. HMBC spectrum of oversilylated β -CD derivative (600 MHz, CDCl_3 , 298 K). Depicted structure is tentative.



Supplementary Figure 49. ROESY spectrum of oversilylated β -CD derivative (600 MHz, CDCl_3 , 298 K). Depicted structure is tentative.

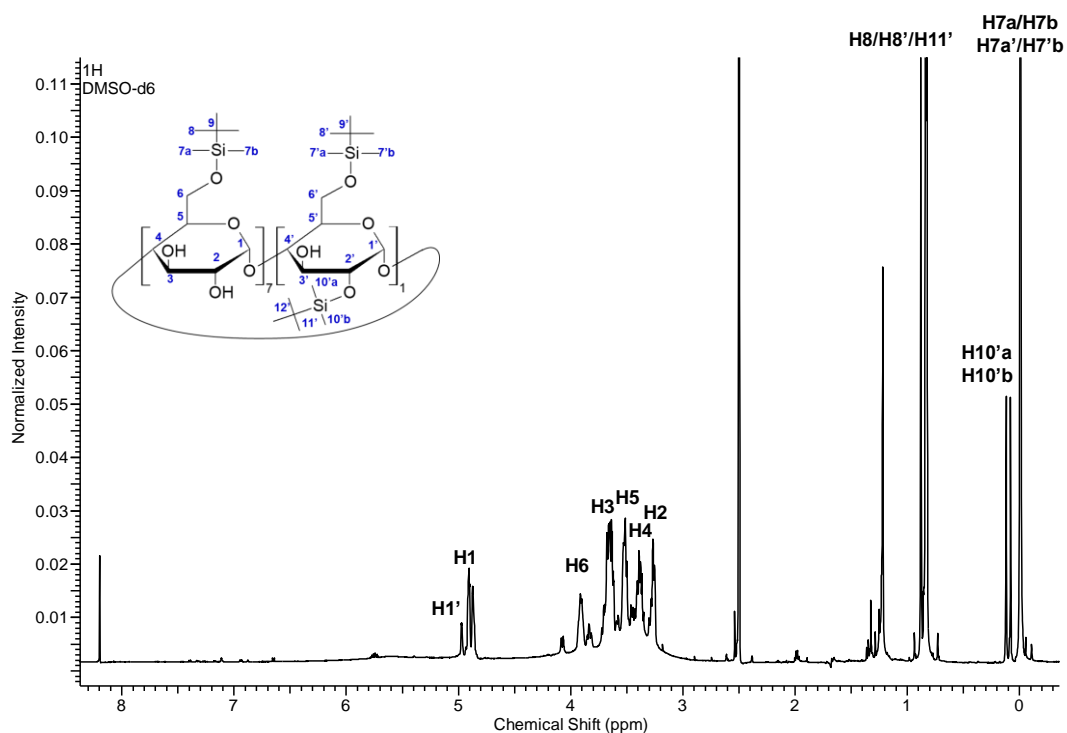


Supplementary Figure 50. MALDI spectrum of oversilylated β -CD derivative (DHB as matrix). Depicted structure is tentative.

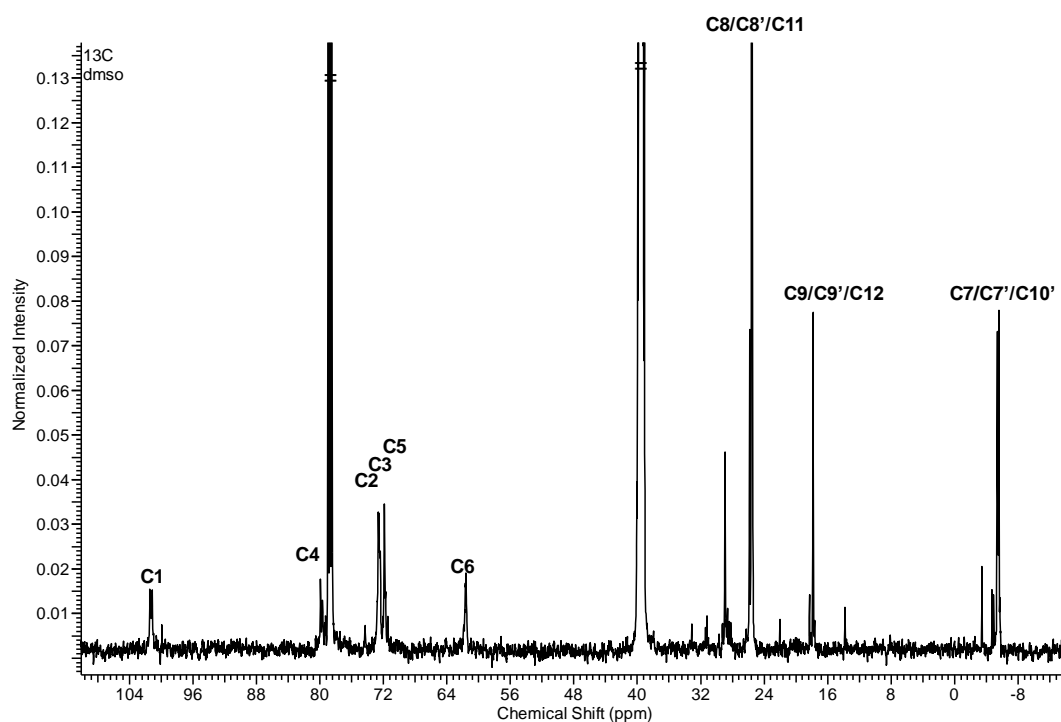


Supplementary Figure 51. IR spectrum of oversilylated β -CD derivative (KBr disk). Depicted structure is tentative.

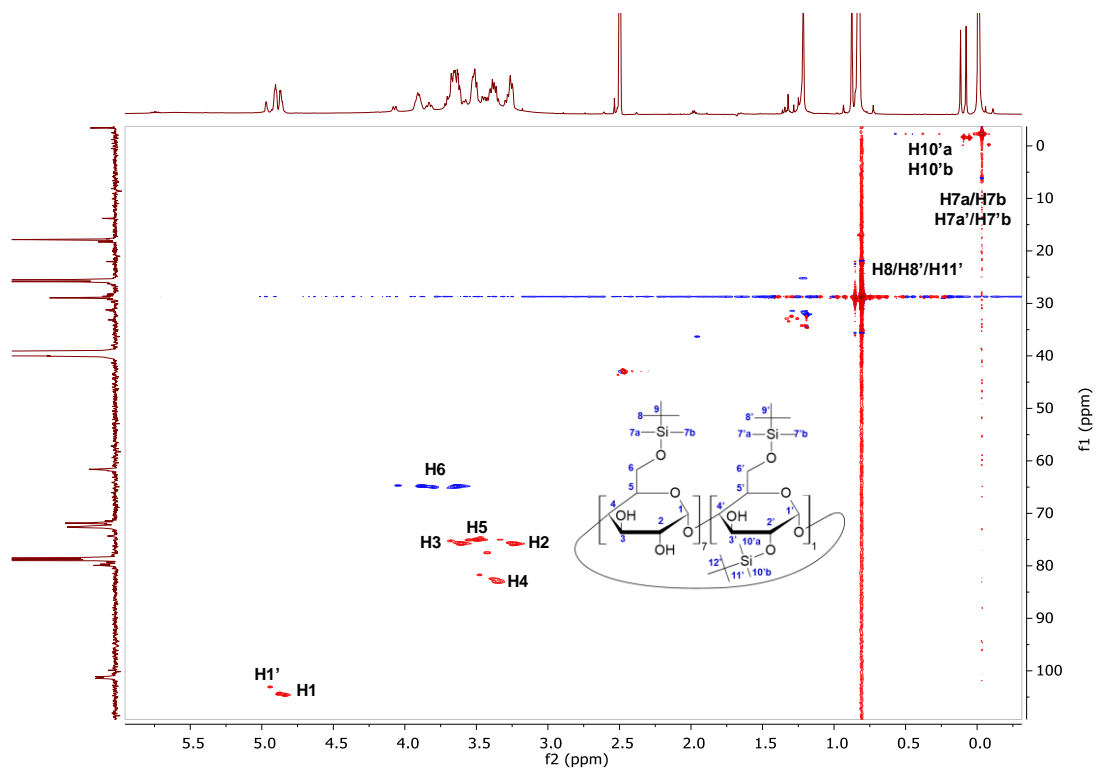
XII. NMR, MALDI and IR spectra for oversilylated γ -CD derivative



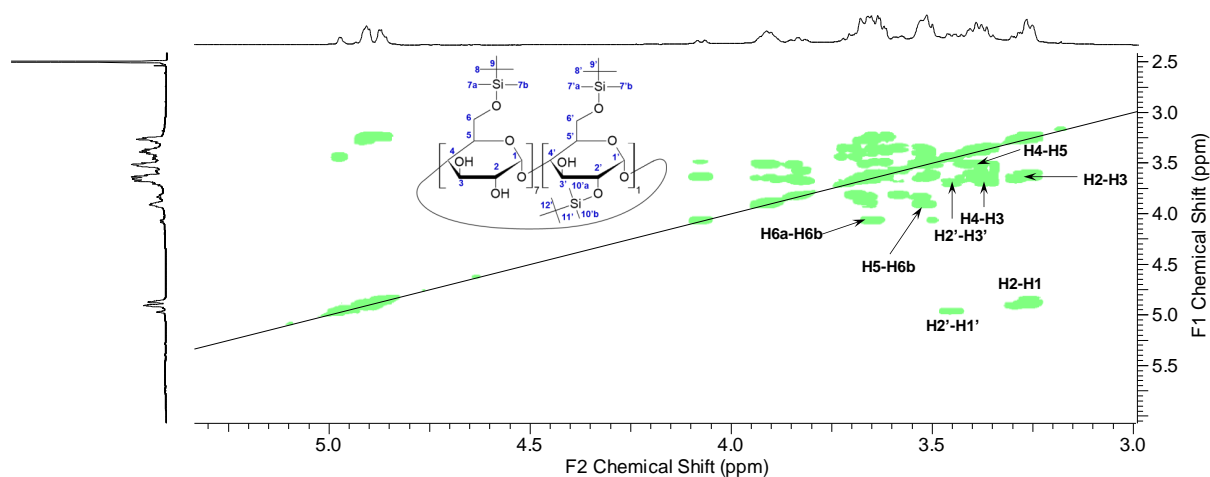
Supplementary Figure 52. ^1H spectrum of oversilylated γ -CD derivative (600 MHz, DMSO-d_6 : CDCl_3 3:1, 298 K) with partial assignment. Depicted structure is tentative.



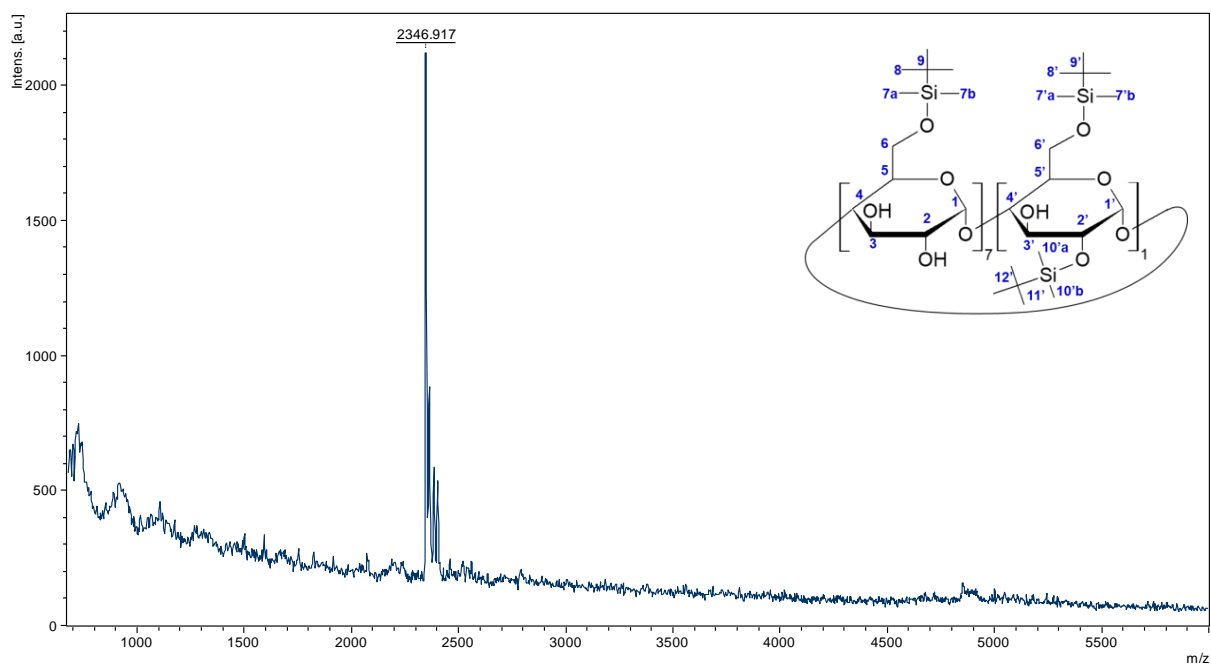
Supplementary Figure 53. ^{13}C spectrum of oversilylated γ -CD derivative (150 MHz, DMSO-d_6 : CDCl_3 3:1, 298 K) with partial assignment. Depicted structure is tentative.



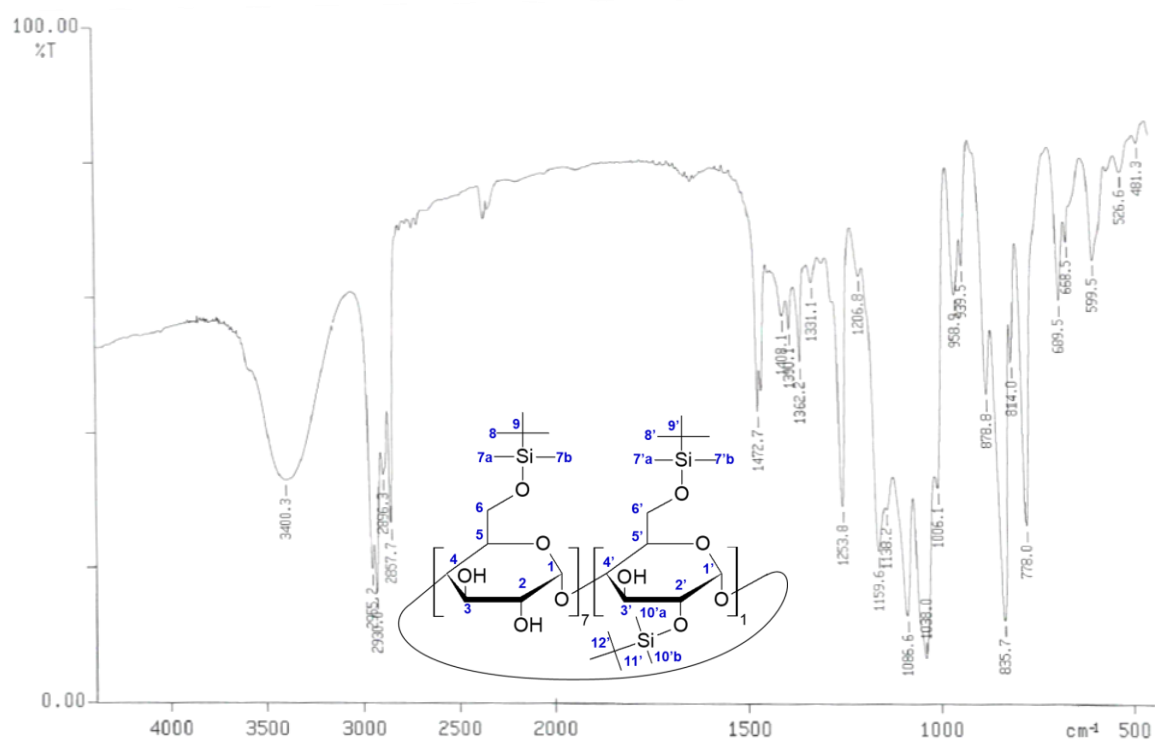
Supplementary Figure 54. DEPT-edited HSQC spectrum of oversilylated γ -CD derivative (600 MHz, DMSO- d_6 :CDCl $_3$ 3:1 298 K) with partial assignment. Depicted structure is tentative.



Supplementary Figure 55. COSY spectrum of oversilylated γ -CD derivative (600 MHz, DMSO- d_6 :CDCl $_3$ 3:1, 298 K) with partial assignment. Depicted structure is tentative.



Supplementary Figure 56. MALDI spectrum of oversilylated γ -CD derivative (DHB as matrix). Depicted structure is tentative.



Supplementary Figure 57. IR spectrum of oversilylated γ -CD derivative (KBr disk). Depicted structure is tentative.